A Sliding Window Decorrelating Receiver for Multiuser DS-CDMA Mobile Radio Networks

S. S. H. Wijayasuriya, *Member, IEEE*, G. H. Norton, and J. P. McGeehan

***Abstract*—In this paper we detail the development of a near–far (NF) *resistant* sliding window decorrelating algorithm (SLWA) that overcomes the near-far problem (NFP) pertaining to the conventional linear correlation receiver (CLCR) and alleviates some of the limitations of the standard decorrelator [1]. The SLWA architecture is extended to incorporate differentially coherent multipath (RAKE) diversity combining techniques and hence achieves simultaneous rejection of multiuser and multipath interference. This paper also presents a novel algorithm for the updating of decorrelator coefficients using a fully parallel architecture. We present a mathematical model for the performance of a sliding window scheme, the main contribution of which is the analysis of finite sequence length multipath decorrelation under the practical limitation of incomplete RAKE combining. In addition to numerical results, we present results pertaining to capacity improvements achieved over the CLCR, derived from a simulation of a multiuser direct-sequence code-division multiple-access (DS-CDMA) mobile radio system.**

I. Introduction

IN RECENT years, direct-sequence code-division multiple-access (DS-CDMA) has been actively considered as a candidate-access technique for future generation mobile radio systems. With the resurgence of interest in this technique for commercial application, the near-far problem (NFP) has been generally accepted as the principal shortcoming of conventional DS-CDMA reception techniques, with respect to a mobile radio environment. The first DS-CDMA prototype systems have been recently commissioned in the United States [2] and use a closed-loop power control strategy to overcome the NFP. As will be discussed, this solution approach has many limitations, including the feasibility at practical vehicle speeds [3], [4]. Much research has, therefore, been directed toward the development of near–far (NF) resistant receivers. Of the alternative strategies proposed in the literature, the decorrelation concept has emerged as the most attractive for a centralized base station solution, given the dynamic nature of the mobile radio channel. As will be shown in this paper, however, the standard decorrelator proposed by [1] has many shortcomings that inhibit practical implementation. In this paper we propose a sliding window decorrelating algorithm (SLWA) that alleviates many of the shortcomings (complexity issues and otherwise) of the standard decorrelator, while achieving the same asymptotic performance. There is, however, a restriction on the applicability of the SLWA in that the transmit data has to be encoded using a convolutional error correcting code. This requirement is discussed further in Section II. It follows that the algorithm cannot be used in conjunction with arbitrary uncoded DS-CDMA data transmissions.

It has been established [1], [5]–[7], that the NFP is an inherent shortcoming of the CLCR and not of the DS-CDMA concept itself. Contrary to traditional interpretation, the NF problem (as the term may imply) does not originate solely from differences in propagation loss. In a cellular-type mobile radio environment, the impact of multiuser interference, as perceived by a single-user detector, can be attributed to the following effects: 1) propagation loss and shadowing, 2) fast fading and 3) multipath propagation in a time-dispersive channel. It is conceivable that effect 1) can be easily ameliorated using a slow or open-loop power control strategy. Multipath fading effects, however, result in the received signals along multiple paths exhibiting independent fast fading. From a power control point of view, the latter source of received energy variation poses a much more complex problem than that due to shadowing (slow fading) or propagation loss. Here we reiterate the views of Turin [8], who stressed the devastating effects of fast fading and multipath propagation as a variant of the classical NFP, and the concerns expressed by researchers [4], [8] regarding the feasibility and success of rapid power control strategies at practical vehicle speeds.

The organization of the paper is as follows. In Section II we outline the multiuser reception problem, basing the discussion on the multiuser DS-CDMA communication model [9]. After a brief review of other solutions to the near–far problem proposed in the literature with particular emphasis on the linear time invariant (LTI) decorrelator, we proceed to develop the SLWA. In Section III, we dwell briefly on the mobile radio communication channel and extend the SLWA to a differentially coherent multipath (RAKE) decorrelator. The performance of the receiver is evaluated by simulation and capacity comparisons made with the conventional linear correlation receiver (CLCR). In Section IV, a novel algorithm is proposed for the updating of decorrelator coefficients in response to changes in the multiuser configuration and processing requirements estimated. Section V is devoted to a mathematical model for the bit error rate (BER) performance of a sliding window decorrelator in AWGN and multipath fading channels. Finally, in Section VI conclusions are drawn from the work presented in this paper.

II. A Sliding Window Decorrelating Algorithm

Consider the problem of the mobile-to-base station (reverse) link in a multiuser network. The source of the NF problem lies in the fact that the CLCR output possesses a spurious

Manuscript received August 18, 1993; revised May 2, 1994.

The authors are with the University of Bristol, Centre for Communications Research, Bristol BS8 1TR, UK.

Publisher Item Identifier S 0018-9545(96)00951-6.

component linear in the amplitude of each of the interfering users.

A. Multiuser DS-CDMA Model

References [1], [5], and [9] describe the multiuser communication model that is the basis for the class of linear detectors and the standard (LTI) decorrelator defined by [1]. The algorithm developed in this paper is designed to alleviate some of the shortcomings of the LTI decorrelator.

B. Terminology

Let us consider a system consisting of K users and a transmission of arbitrary length N. Let $b_k(i)$, $w_k(i)$, $y_k(i)$, and $s_k(t)$ be respectively the ith data bit, the received energy of this data bit, corresponding matched filter output, and signature waveform of the kth user. Let $n(t)$ be the AWGN. We consider a K user system and denote the symbol period by T. Assume the users are numbered according to their delays τ_i, so that $0 \le \tau_1 \le \tau_2 \cdots \le \tau_K < T$. Also define

$$\tilde{s}_k(t) = \begin{cases} s_k(t), & \text{if } 0 \le t \le T \\ 0, & \text{otherwise.} \end{cases} \tag{1}$$

C. Discrete Time Model

The CLCR output $y_k(i)$ can be written

$$y_k(i) = S_1 + S_2 + S_3 \tag{2}$$

where

$$\begin{aligned} S_1 &= \sum_{i=1}^{M} \int_{-\infty}^{\infty} b_k(i)\sqrt{w_k(i)}\tilde{s}_k(t - iT - \tau_k) \\ &\quad \cdot \tilde{s}_k(t - lT - \tau_k)\, dt \\ S_2 &= \sum_{i=1}^{M} \sum_{\substack{j=1 \\ j \ne k}}^{K} \int_{-\infty}^{\infty} b_j(i)\sqrt{w_j(i)}\tilde{s}_j(t - iT - \tau_j) \\ &\quad \cdot \tilde{s}_k(t - lT - \tau_k)\, dt \\ S_3 &= \int_{-\infty}^{\infty} n(t)\tilde{s}_k(t - lT - \tau_k)\, dt. \end{aligned}$$

Let $R(l)$ be the $K \times K$ normalized signal crosscorrelation matrices such that

$$R_{k,j}(l) = \int_{-\infty}^{\infty} \tilde{s}_k(t - \tau_k)\tilde{s}_j(t - lT - \tau_j)\, dt. \tag{3}$$

It follows that

$$R(l) = 0 \quad \text{for } |l| > 1; \quad R(-l) = R^T(l). \tag{4}$$

We use a vector notation for the matched filter outputs, transmit data, and noise (e.g., $\boldsymbol{y}(l) = [y_1(l), y_2(l), \cdots, y_K(l)]$), and also define a received energy matrix

$$W(l) = \text{diag}\,(\sqrt{w_1(l)}, \sqrt{w_2(l)}, \cdots, \sqrt{w_K(l)}). \tag{5}$$

S_1 of (2) is the term we seek for the kth user. S_2 is the multiple access (MA) interference comprising interference from $l+1$th, lth and $l-1$th bits of other users, and S_3 the thermal noise. The matched filter output can be written as the output of a discrete time model

$$\begin{aligned} \boldsymbol{y}(l) = R(-1)W(l+1)\boldsymbol{b}(l+1) + R(0)W(l)\boldsymbol{b}(l) \\ + R(1)W(l-1)\boldsymbol{b}(l-1) + \boldsymbol{n}(l) \end{aligned} \tag{6}$$

where $\boldsymbol{n}(l)$ is the matched filter output noise vector at time instant $t = lT$ with autocorrelation matrix given by

$$E[n(i)n^T(j)] = \sigma^2 R(i-j). \tag{7}$$

The partial correlation matrices can be computed from information available at the base station, or tabulated for moderate code sets and lengths [10]. The table should be indexed by the pair of interfering codes and the relative delay.

D. Solutions to the Near–Far Problem

Much of the work on multiuser detection has been motivated by the work of Verdu [5] who shows that the performance to be gained by optimum demodulation, over the CLCR is very significant. From a practical and commercial perspective, the research into near–far resistant detection is also motivated by the skepticism regarding the feasibility of rapid power control [2], [4], [8] at practical vehicle speeds. Solutions proposed in the literature can be classified as follows. Probabilistic methods include the optimum multiuser detector [5] and the sequential decoding algorithm proposed in [6]. The complexity of these algorithms precludes their application in a mobile-radio-type application. In particular, the complexity of the optimum detector increases exponentially with the number of users in the system. Another class of multiuser interference cancellation algorithm includes detectors that employ the principles of postcorrelation and precorrelation interference regeneration and cancellation. Multistage postcorrelation detection has been proposed in [7] and [11], and is motivated by the fact that restricting the decision statistics to be linear functions of the sufficient statistics, as in the case of decorrelating solutions, is not optimum for the detection of weak signals. Precorrelation (successive) interference cancellation [12]–[14] offers a complexity advantage over postcorrelation techniques, since each user needs to be canceled only once. Both postcorrelation and precorrelation interference cancellation techniques require accurate knowledge of received energies. This requirement is a stringent one in mobile radio channels where rapid fluctuations need to be tracked accurately in the presence of multiuser interference. Lupas and Verdu [1] and [15] pioneered the work on linear detectors and, in particular, developed the LTI decorrelator. An important feature of the decorrelator is the fact that it does not require knowledge of received energies. In fact, the decorrelator is the maximum likelihood detector when the received energies are unknown. A decision feedback decorrelator for synchronous DS-CDMA channels is proposed in [16], which combines the ideas of decorrelation and successive cancellation. Here, too, the limitations of the decorrelator with respect to weaker signals is recognized, and a solution is proposed that is optimum with respect to the detection of such signals, provided accurate estimates of received energies are available. A scheme for received energy estimation based

on linear predictive principles is proposed in [16]; however, it is conceded that the decision-feedback scheme must revert to standard decorrelation under circumstances where received energies are too rapid to be modeled as a linear combination of past estimates. The frequency with which such a scenario might arise in a multipath fading environment has not been established. The solution proposed also uses a noise-whitening process that renders the thermal noise components in the decision statistics uncorrelated, with resulting improvements in performance, especially under low SNR.

We work from the rationale that for a multiuser mobile radio application, it is prudent to assume that received energies and phases are unknown. Such a scheme will not be dependent on the feasibility of implementing a subsystem that is capable of tracking energies of all users and multipaths in the presence of multiuser interference. Furthermore, complexity issues are important. The computations required by an algorithm can be separated into overhead (or setup) and per-iteration components. The latter will be reflected in system processing delays, whereas the former can be performed off-line. It is, hence, necessary to minimize per-iteration operations. Competing algorithms to the decorrelator (e.g., interference regeneration and cancellation algorithms [11]–[14]) have high per-iteration cost with most operations being performed at every symbol interval. In this respect a decorrelating algorithm is probably the most inexpensive multiuser detection technique to implement on a per-symbol basis [17] and is analogous to applying a zero forcing equalizer to the CLCR outputs. There is, however a significant cost of recomputation (setup) of the linear system solution. Complexity issues are discussed further in Section IV. Based on the above, it is necessary to begin with the standard decorrelator, as proposed by [1]. The detector is shown to have several short comings with respect to a mobile radio application, which motivates the development of a finite sequence length decorrelating algorithm that achieves the same asymptotic performance as the standard decorrelator.

E. The Linear Time Invariant Decorrelator

We target our decorrelating algorithm at MA limited channels where the dominant source of interference is the presence of multiple users rather than thermal noise. From the definition of near-far resistance (NFR) [1], it is clear that a receiver is NF-resistant, provided there is no irreducible probability of error due to the presence of interfering users.

Assuming an infinite length transmission, Lupas and Verdu [1] propose an LTI filter implementation of the decorrelation process. The filter has transfer function

$$G(z) = \frac{1}{\det(S(z))}\operatorname{adj}(S(z)) \tag{8}$$

where

$$S(z) = R^T(1)z + R(0) + R(1)z^{-1}. \tag{9}$$

Since each element of $S(z)$ will be a polynomial of the form $az^{-1} + b + cz$, the solution involves inverting a $K \times K$ matrix, the elements of which are second-order polynomials in z. The resulting filter is noncausal, and its existence for all combinations of user codes and timing cannot be guaranteed [1]. The complexity of filter derivation makes recomputation of the linear system computationally expensive. It follows that the standard decorrelator is inflexible to changes in the system (e.g., new users in the system, timing drift, multipath selection, or voice activity exploitation), which result in changes in the cross-correlation coefficients. Furthermore, the IIR filter formualtion involves considerable processing delay in order to maintain accuracy (truncation of IIR filter coefficients). These shortcomings of the standard decorrelator inhibit application in a mobile radio environment and motivate the development of the SLWA. Using an infinite length assumption (as in the LTI case) places no demands on the cooperation among multiple mobile users in the system. A finite sequence length formulation in contrast implies that no data is transmitted for one bit period by any user in the system prior to or following the data block, thereby rendering the system memoryless outside the block transmitted. In the case of a practical mobile radio network, this would demand a high degree of cooperation among users, which in turn would place unacceptable demands on the networking protocols. The finite sequence length decorrelation problem can be formulated as in [18]

$$\boldsymbol{Y} = \mathfrak{R}\mathcal{W}\boldsymbol{b} + \mathcal{N}. \tag{10}$$

The terms of (10) are expanded in (11) below (setting $M = 0, N = N$). $\mathfrak{R}$ is an $NK \times NK$ matrix, the inversion of which is not feasible for practical sequence length (N) values. $\mathfrak{R}$ however, is block tridiagonal, and this property can be exploited.

F. Development of SLWA

The objective of the proposed scheme is to apply finite sequence length decorrelator theory to a data transmission of infinite length. In so doing, we combine the virtues of lower computational requirement, and the block tridiagonal system matrix, with the minimal user cooperation requirements associated with an infinite length transmission assumption. Our strategy is to partition the infinite sequence into blocks of size $\acute{N}$. Here $\acute{N}$ is such that the solution of the linear system for a particular left-hand side (LHS) is feasible within a time period of the order of one symbol period. First, define a valid linear system that can be solved within a finite data window. Equation (10) can be written using M, which represents the offset of the beginning of the current window from the start of the sequence

$$\begin{bmatrix} \boldsymbol{y}(M+1) \\ \boldsymbol{y}(M+2) \\ \boldsymbol{y}(M+3) \\ \vdots \\ \boldsymbol{y}(M+\acute{N}) \end{bmatrix} = \begin{bmatrix} R(0) & R(-1) & 0 & \cdots & 0 \\ R(1) & R(0) & R(-1) & \cdots & 0 \\ 0 & R(1) & R(0) & \ddots & 0 \\ \vdots & \vdots & \ddots & \ddots & \vdots \\ 0 & \cdots & \cdots & R(1) & R(0) \end{bmatrix} \cdot \mathcal{W} \begin{bmatrix} \boldsymbol{b}(M+1) \\ \boldsymbol{b}(M+2) \\ \boldsymbol{b}(M+3) \\ \vdots \\ \boldsymbol{b}(M+\acute{N}) \end{bmatrix} + \mathcal{N} \tag{11}$$

where

$$\mathcal{N}^T = [\boldsymbol{n}(M+1), \boldsymbol{n}(M+2), \boldsymbol{n}(M+3), \cdots, \boldsymbol{n}(M+\acute{N})]$$

and

$$\mathcal{W} = \text{diag}\,[W(M+1), W(M+2), W(M+3), \cdots, \cdot W(M+\acute{N})].$$

The linear system (11) is invalid as it stands (unless $M=0$), since according to the discrete time model (6). $\boldsymbol{y}(M+1)$ contains an interference component determined by $\boldsymbol{b}(M)$, and similarly for $\boldsymbol{y}(M+\acute{N})$ and $\boldsymbol{b}(M+\acute{N}+1)$. If a continuous valued transmit data vector is defined

$$\boldsymbol{WB}(i) = [\sqrt{w_1(i)}b_1(i), \sqrt{w_2(i)}b_2(i) \cdots \sqrt{w_K(i)}b_K(i)]$$

it is clear that the required correction terms are $R(1)\boldsymbol{WB}(M)$ in the case of $\boldsymbol{y}(M+1)$, and $R(-1)\boldsymbol{WB}(M+\acute{N}+1)$ in the case of $\boldsymbol{y}(M+\acute{N})$. A modified input vector X is now defined

$$\boldsymbol{x}(M+1) = \boldsymbol{y}(M+1) - R(1)\boldsymbol{WB}(M)$$

$$\boldsymbol{x}(M+\acute{N}) = \boldsymbol{y}(M+\acute{N}) - R(-1)\boldsymbol{WB}(M+\acute{N}+1)$$

$$\boldsymbol{x}(M+i) = \boldsymbol{y}(M+i) \text{ for } 1 < i < \acute{N}. \tag{12}$$

The problem has been reduced to one of obtaining reasonable estimates of the terms $\boldsymbol{WB}(M)$ and $\boldsymbol{WB}(M+\acute{N}+1)$, and solving the linear system $\boldsymbol{X} = \mathfrak{R}\mathcal{W}\boldsymbol{b} + \mathcal{N}$, $\mathfrak{R}$ block tridiagonal.

1) Estimation of Edge Correction Terms: Provided the receiver is initialized in a suitable manner, $\boldsymbol{WB}(M)$ is clearly available from the previous iteration. This provides an exact estimate when the noise power spectral density (PSD) is zero, thus satisfying the NF resistant condition. We next consider the prediction of unexplored data. Since we assume that MA interference is the dominant source of interference and underpins our investigation, we cannot approximate $\widehat{\boldsymbol{WB}}(M+\acute{N}+1)$ by $\boldsymbol{y}(M+\acute{N}+1)$. Several finite sequence length decorrelator architectures are proposed in [19]. Estimation of unexplored data is of crucial importance in a asynchronous system. The solutions proposed in [19] are based on using the matched filter output to estimate unexplored data. The performance degradation due to using this approach, especially under multiple access limited conditions, is shown in Figs. 9 and 10. We use the notation $\hat{\boldsymbol{W}}(.)$ and $\hat{\boldsymbol{b}}(.)$, as it is necessary to make independent estimates for these vectors. Linear predictive methods have been used [20] for the prediction of fading envelopes. It was found, however, that the added complexity was not justified by the marginal gain in perfromance. We prefer to use $\boldsymbol{W}(M+\acute{N}+1) \approx \hat{\boldsymbol{W}}(M+\acute{N}-1)$ because it is simple to implement and sufficiently accurate under most fading conditions. Next, we focus on the prediction/estimation of future data bit values, i.e., $\boldsymbol{b}(M+\acute{N}+1)$. For reasons already discussed a simple solution based on the CLCR approximation $\hat{\boldsymbol{b}}(M+\acute{\boldsymbol{N}}+1) = \text{sgn}\,(y(M+\acute{N}+1))$ introduces an element of NF dependence. Hence, we propose a solution that identifies a novel use for the predictive properties of a noncatastrophic convolutional code that possesses the trellis path uniqueness (TPU) property [10], and [21].

2) Prediction Using Convolutional Coding: The problem at hand is the requirement to be able to predict the polarity of future data based on the polarity of received data. This requires that the received data transmission have some deterministic structure. Convolutional encoding is performed by a finite state machine and could be described as possessing this property. If this structure can be identified and exploited to provide predictive capability, the redundancy associated with error correction coding will serve the dual purpose of aiding the prediction as well as providing error correcting capability at the next stage of the receiver.

The required property has been identified empirically [10], [18], and supported with algebraic analysis [21]. The predictive property that arises from the uniqueness of trellis paths associated with encoded sequences (TPU property; see [10], [21]), can be defined as follows.

Property 2.1: For a code of constraint length $m+1$ and code rate $R = 1/n$, observing m consecutive sets (n bits) of outputs (nm bits), uniquely defines a path connecting $m+1$ states, and hence uniquely defines the current $(m+1)^{st}$ state on this path. If the next bit of output is also known, this path uniquely determines the next $n-1$ output bits.

A look-up table indexed by history data can be used to provide efficient prediction. This and other features and applications of the prediction algorithm and TPU property are discussed in detail in [10], and [21].

The prediction does not rely on a decision made by the conventional detector and, in this respect is independent of the relative energies of the users. From here on we consider a rate 1/2 code for the decorrelating application. As discussed in [18], a two-stage prediction is required. It is important to note that the predictive property can be applied once every encoded symbol (two bits in the case of a half rate code). In the case of the SLWA, this is easily accommodated by sliding the window by two vectors each iteration. It is, however, necessary to position the data within the window so that the required history data is always available to the prediction algorithm. Convolutional interleaving is used to achieve this. In order to simplify the notation, we denote the (half rate) encoder outputs as $A(1):A(2)$, $B(1):B(2)$, and so on, $A, B, \cdots$ represent output symbols with the index within the parenthesis representing the bits within the symbol. For this example, we use a window length of 6. Fig. 1 shows schematically the contents of a window (after interleaving) at a particular instant in time. The prediction involves two steps: 1) predict $F(2)$ using $F(1)$, $E(1)$, $E(2)$, $D(1)$, $D(2)$, followed by 2) predict the required $G(2)$ from $G(1)$, $F(1)$, $F(2)$, $E(1)$, $E(2)$.

We now have all the information required to perform the edge correction. It is important to note that the edge correction strategy is independent of the transmissions of other users and their relative energies. Perfect edge correction is achieved in the absence of thermal noise. It follows that there is no irreducible error rate due to the presence of multiple users in the system, and the algorithm is near–far resistant by definition [1]. Finally, to solve the linear system

$$\boldsymbol{X} = \mathfrak{R}\mathcal{W}\boldsymbol{b} + \mathcal{N} \tag{13}$$

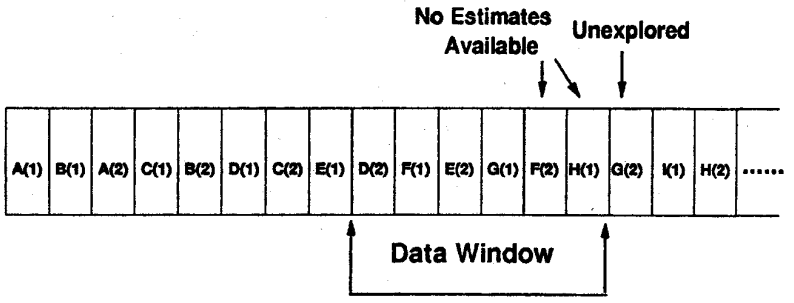

Fig. 1. Contents of a decorrelating window.

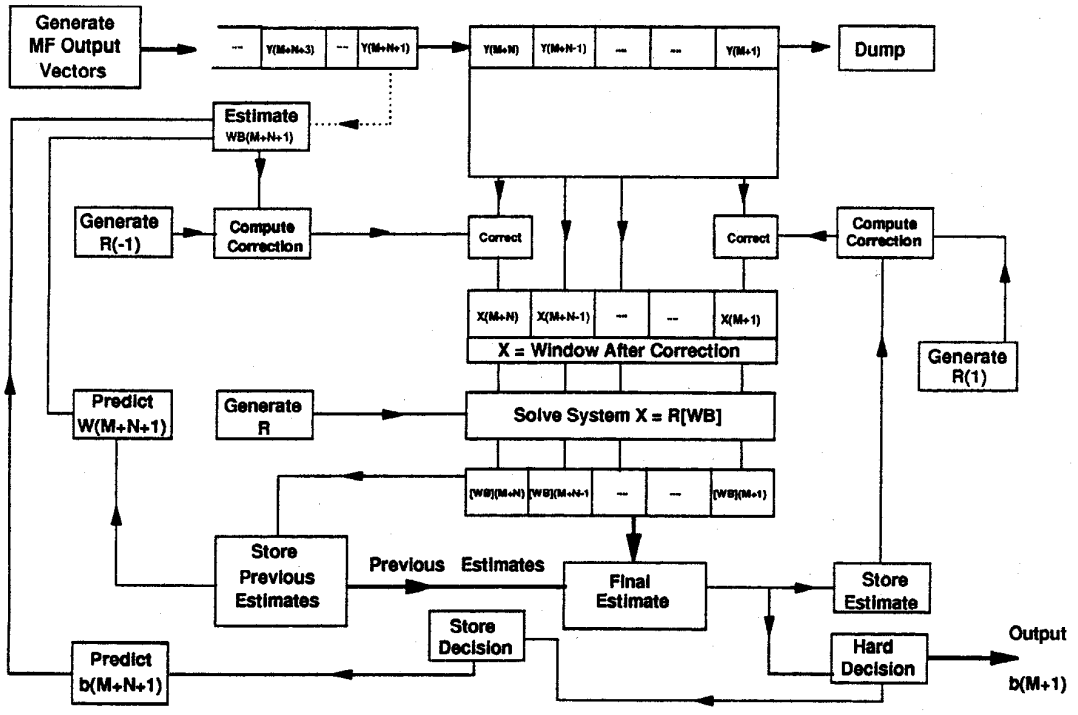

Fig. 2. Sliding window decorrelating algorithm.

the block tridiagonal structure of $\mathfrak{R}$ can be exploited by using LU decomposition to reduce the solution to the following recurrences

$$\begin{aligned} Z_1 &= R(0)^{-1}R(-1) \\ Z_k &= (R(0) - R(1)Z_{k-1})^{-1}R(-1) \\ &\qquad k = 2, 3 \cdots \acute{N} \\ \boldsymbol{W_1} &= R(0)^{-1}\boldsymbol{y}(M+1) \\ \boldsymbol{W_k} &= (R(0) - R(1)Z_{k-1})^{-1}(\boldsymbol{y}(M+k) \\ &\qquad - R(1)\boldsymbol{W_{k-1}}) \\ &\qquad k = 2, 3 \cdots \acute{N} \\ \boldsymbol{WB}(M+\acute{N}) &= W_{\acute{N}} \\ \boldsymbol{WB}(M+k) &= W_k - Z_k\boldsymbol{WB}(M+k+1) \\ &\qquad k = \acute{N}-1, \acute{N}-2 \cdots 1. \end{aligned} \tag{14}$$

Fig. 2 is a schmatic representation of the proposed algorithm.

G. Near–Far Resistance of SLWA

From the above, it is clear that our algorithm is NF-resistant by definition by virtue of an edge-correction strategy that is independent of user energies in the absence of thermal noise. We also confirm NF-Resistance by simulating a multiuser asynchronous DS-CDMA system in AWGN. Fig. 3 shows results obtained using Gold Codes of length 127. To represent a simple NF situation, one of the interferers transmits at 0, 20, and 40 dB relative to the level of the desired user NFR of 0, 20, and 40 dB. The other users in the system have the same received SNR as the desired user. It is assumed that perfect timing with regard to sampling the matched filter output at each data bit interval is obtained. The bit-error-rate (BER) of the SLWA is reduced to zero in the absence of thermal noise, irrespective of the number of users in the system or the power of the strong interferer. NF resistance is hence established. The performance of the CLCR is seen to be affected drastically by the power level of the strong interferer. Performance at

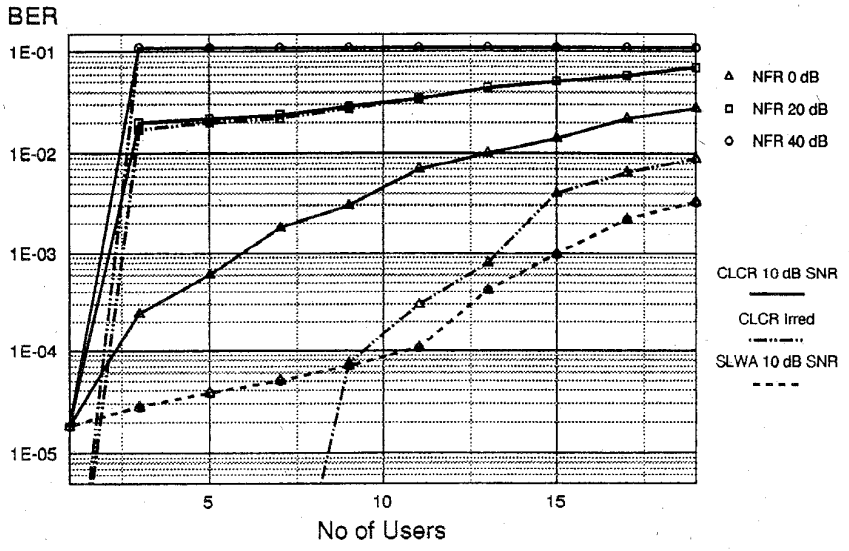

Fig. 3. Performance in AWGN channel with strong interferer (simulation).

an operating SNR is also shown. Decorrelation (since it is a zero forcing technique) suffers from noise enhancement [16], and [22] but is insensitive to the number (or energies of) users in the system for the case under consideration. At this stage, it is instructive to compare the performance of the SLWA with that of other detection strategies proposed in the literature [1], [7], [16]. The performance of the decorrelator, CLCR, multistage, optimum, and optimum linear receivers for the bandwidth-efficient two-user case and for a system with spreading factor (SF) 7, and four users is given in Figs. 2 and 5(d) of [7] respectively. The performance of the decision feedback decorrelator for the same cases is given by Figs. 2 and 3 of [16]. We evaluate the performance of the SLWA by simulation for the same scenarios in Fig. 4. For the four-user case, the same Gold sequences as those in [7] and [16] are used. It was verified that for synchronous DS-CDMA (assumed in [7] and [16]), the performance of the SLWA was identical to that of the decorrelator since no edge correction is involved. The curves of Fig. 4 are for the asynchronous case. The performance of the SLWA deviates from the decorrelator when the number of edge correction errors (increase when SNR of interferes is low) and their impact (increase when relative SNR of interferes is high) becomes significant. It is important to note the impact of relative energies on SLWA performance in the case of a bandwidth-efficient configuration. This is in contrast to the relatively lightly loaded case depicted by Fig. 3 where the NFR curves for the SLWA coincide for the 10 dB case. It is clear from a comparison with the results of [7], and [16] that the multistage receivers and decision feedback decorrelator provide superior performance in the case of the detection of weaker users. It must be noted, however, that these techniques assume knowledge of received energies that the SLWA does not.

It is not possible to investigate bandwidth-efficient scenarios for large user configurations because of prohibitive simulation time. The performance under such conditions for AWGN and fading channels is evaluated using the mathematical model of

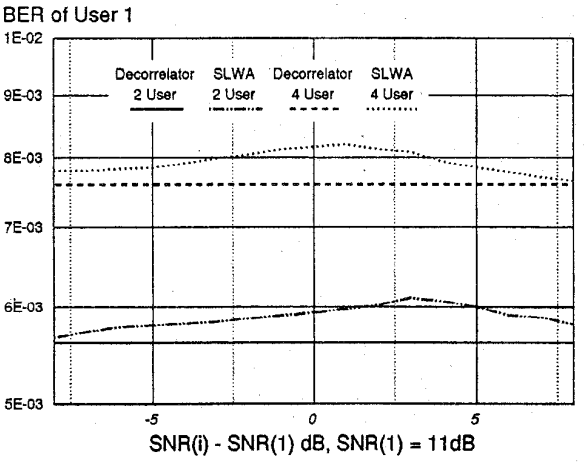

Fig. 4. Comparison (SLWA simulated) with decorrelator for bandwidth efficient channels.

Section IV in Figs. 19 and 22. The SLWA clearly offers large capacity improvements over the CLCR when the channel is MA limited, the improvements being more significant in an NF situation.

III. Multiuser Detection in Fading and Mobile Radio Channels

Consider a multiuser mobile radio environment. Fading, oscillator phase instability at transmitter and the dynamically evolving positions of transmitter and receiver are factors that preclude the use of coherent communication in a single-user environment. In a multiuser environment, the tracking has to be performed in the presence of multiuser interference in addition to that due to other sources. The above factors hence prove to be even stronger deterrents to coherent communications in a multiuser environment. We hence follow [23] in proposing that the SLWA be applied in conjunction

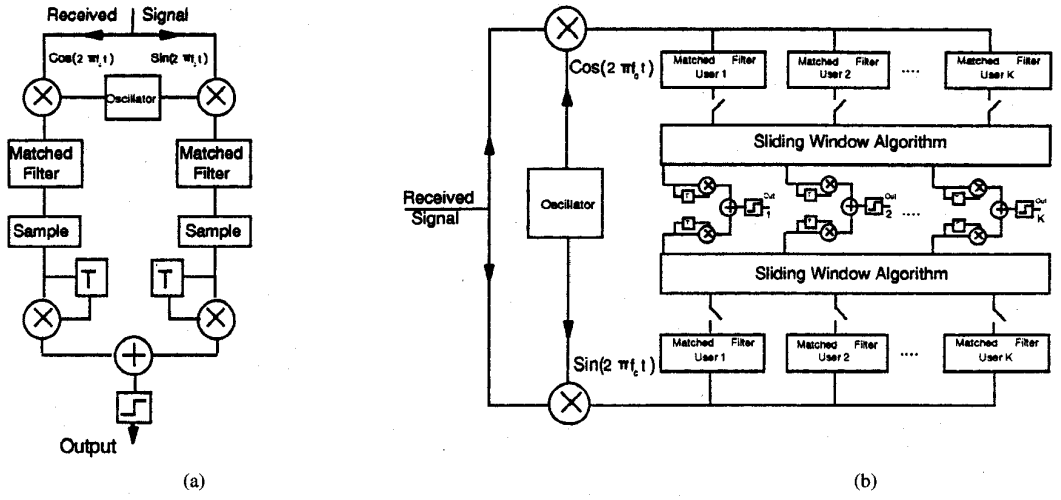

Fig. 5. (a) Single-user B-DPSK CLCR receiver. (b) Multiuser B-DPSK SLWA receiver.

with a differentially coherent modulation scheme. In such a receiver structure, no knowledge of user-received energies or phases will be required. It must be noted, however, that the scheme (as does any multiuser detection scheme) relies on the underlying assumption that the timing point for the sampling of the matched filter outputs can be accurately determined, even in a multiple-access limited channel. A simple solution aimed at low-signal to interference conditions is proposed in [14]. We focus on binary differential phase shift keying (B-DPSK) for CDMA systems. Denoting the quadrature CLCR outputs as y_k^I and y_k^J, we can write [for the CLCR decision statistic as depicted in Fig. 5(a)]

$$\begin{aligned}\hat{b}_k(i) &= \operatorname{sgn}\left[Re\{y_k(i).y_k^*(i-1)\}\right] \\ &= \operatorname{sgn}\left[\{y_k^I(i).y_k^I(i-1) + y_k^J(i).y_k^J(i-1)\}\right]. \quad (15)\end{aligned}$$

In B-DPSK considered here, the same locally generated code is used on both quadrature branches for demodulation. From the above and Fig. 5(a), it is clear that problems with regard to multiuser interference and the NFP would exist independently in the two branches. It is shown in [23] for the synchronous case that the differentially coherent CLCR is not NF resistant. We hence propose that the SLWA be applied in quadrature prior to differential detection. The strategy is shown in Fig. 5(b). Denoting decorrelator outputs on quadrature branches by d^I and d^J, the kth-user decision statistic D_k, for B-DPSK can be written

$$D_k = d_k^I(i).d_k^I(i-1) + d_k^J(i).d_k^J(i-1). \quad (16)$$

By virtue of the decorrelation and the orthogonality of the quadrature channels, the differentially coherent SLWA detection scheme is independent of both the received energies and phases of the multiple users in the system. Using differential encoding, however, impacts the edge correction strategy. The predictive property applies to the convolutionally encoded data (prior to differential encoding), whereas the edge correction must be applied on the received (differentially encoded) data. The modified algorithm is required to differentially decode the index into the look-up table (history data), read off the prediction, and differentially re-encode the predicted data in order to apply the correction [10].

A. Effect of Multipath Fading on DS-CDMA Performance

In a multipath fading environment, we are able to further dissect the factors contributing to the total interference in a multiuser DS-CDMA system, as perceived by a single-user detector. Our discussion on multiuser interference will be based on the interference to the ith user from the jth user. We now consider the factors that could magnify the significance of finite cross correlation between the user codes $c_i(t)$ and $c_j(t)$.

1) Classical Near–Far Effects: The dominant component here is due to the inverse square law propagation loss. Slow fading or shadowing due to obstructions such as large buildings or mountains, can be grouped together with the latter to constitute a slow varying dissimilarity in received power levels often modeled as a log-normal distributed signal. An equivalent static model based on inverse fourth power law attenuation is also used [24]. Slow received energy variations can conceivably be ameliorated by relatively simple open-loop power control strategies.

2) Effect of Fast (Rayleigh) Fading: Fast fading of individual users is independent, and the rate of fading is dependent on the vehicle velocity. This is a rapidly fluctuating variant of the NFP with the added significance that its negation using power control techniques becomes more complex with increasing vehicle speed. Here we investigate the effect of fast fading by simulating independent single path fading links between multiple transmitters and the base station receiver. The propagation environment thus simulated is similar to that found in a suburban area where a single fading link dominates, and relatively little energy is distributed over differential delay multipaths. A multiuser DS-CDMA simulation model has been written. The model uses Gold codes and allows for a capacity comparison of the SLWA and the CLCR in AWGN, fading, and multipath fading channels. For clarity, we have omitted the BER's after decoding the convolutional code. It was verified that the BER of the SLWA was <0.4%, whereas the BER of the CLCR exceeded the error-correcting capability of the half

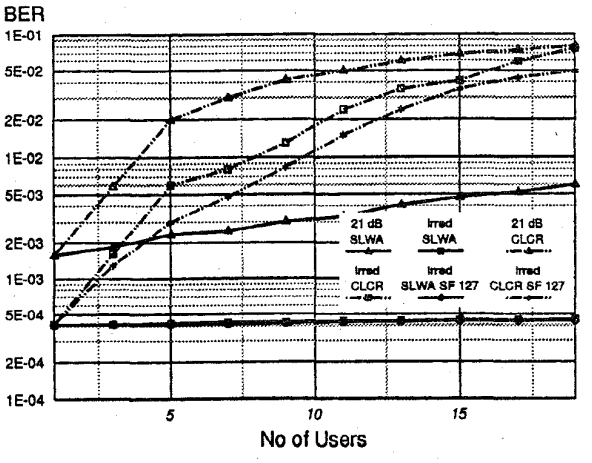

Fig. 6. Single-path fading performance $f_D T_s = 0.005$, for 25.0 dB SNR, and irreducible cases with SF = 63 (simulation).

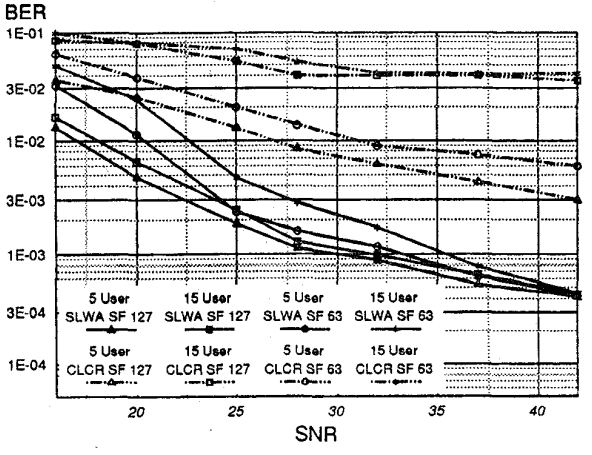

Fig. 7. Effect of SF and loading (simulation).

rate code, in most cases. All simulation and analytical results in this paper are based on all users (other than in a specified NF situation) possessing the same average received energy (hence, average received SNR). This is analogous to assuming that the system has open-loop power control to compensate for long-term signal variations. No compensation for fast fading is assumed. From Fig. 6 it is clear that the SLWA outperforms the CLCR for both thermal noise scenarios. The number of users, or the spreading factor (SF), has little effect on the SLWA irreducible, which deviates only marginally from the single-user case, due to edge-correction errors and Doppler effects. In the presence of noise, the CLCR benefits greatly from the increased SF (Fig. 7). The SLWA also benefits because of reduced interference enhancement, but to a lesser extent than the CLCR. In Fig. 7 the SLWA performance is only marginally dependent on the number of users, unlike in the case of the CLCR, which is in turn relatively insensitive to thermal noise, when it is MA limited. It is clear, however, that the CLCR is rendered unusable in a multiuser system because of fast fading, hence precluding the achievement of bandwidth-efficient MA.

The relative performance of four edge-correction strategies is investigated by simulation in Figs. 9 and 10 for AWGN and

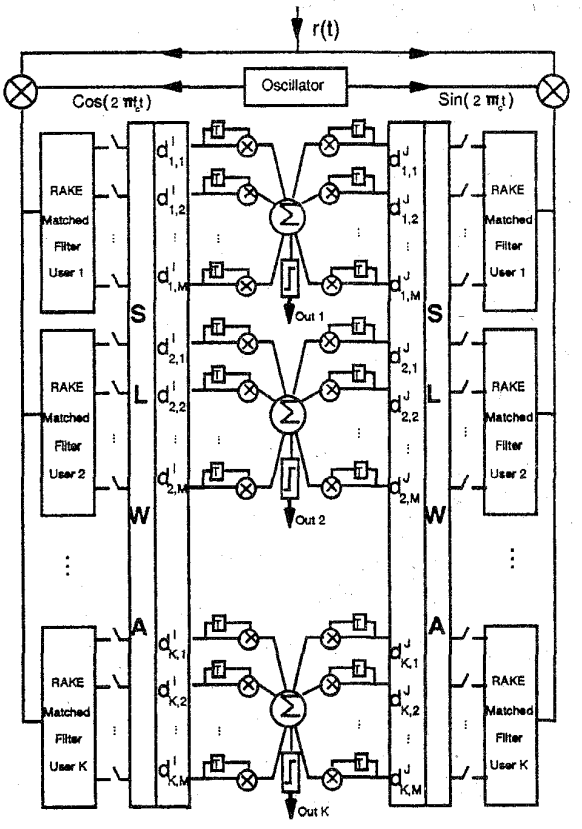

Fig. 8. Multiuser SLWA-RAKE receiver architecture.

Rayleigh fading single-path links, respectively. Simulation of perfect edge correction in a fading channel is computationally very expensive since it involves saving (and recalling) the single-user received waveforms for each of the users being simulated. This precludes the investigation of perfect edge correction in a multipath fading channel. The impact on performance of using the CLCR output as an estimate of the unexplored (edge) data is also shown in Figs. 9 and 10. This provides an indication of the performance degradation suffered by the SLWA relative to an ideal decorrelator. From the curves, it is clear that the SLWA performance is very close to that of perfect edge correction in the low BER regions. It must be noted that a practical voice system will be targeted at this performance region in the first place. The relatively flat irreducible error curves of Fig. 6 indicate that in a fading channel, the effects of nonideal edge correction are negligible in the absence of thermal noise.

B. Multipath Propagation and DS-CDMA

Consider a wide band temporally dispersive channel [25]. In a DS system, a resolution of T_c (chip period) is available in the delay profile. The following channel model based on the agglomeration of rays within a chip period, or resultant paths, is hence more appropriate:

$$h(t;\tau) = \sum_{k=1}^{M} c_k(t)\delta(\tau - kT_c). \tag{17}$$

TABLE I
SUMMARIZED IMPACT OF (INCREASING) SYSTEM PARAMETERS

System Parameter	Residual Energy	Attenuation via PG	Interference Enhancement
Spreading Factor	+	+	-
Combining Depth	-	NA	+
No of Users	+	NA	+

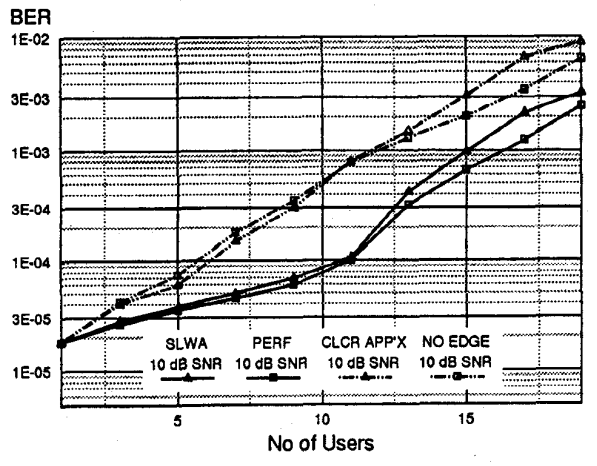

Fig. 9. Impact of edge correction—AWGN.SF 127 (simulated).

For a total delay spread of T_m, M is such that $MT_c >= T_m$, where the $c_k(t)$ are the complex signal variations of each path. It is clear that each additional path in the link connecting the mobile and the base station adds extra interference to an extent determined by the PN code autocorrelation. The multipath activity would also contribute to the interference to other users in the system to an extent determined by the crosscorrelation coefficients. The said multipath situation is true for all users in the system. Conceptually, it is possible to model the multipaths as additional users in the system, each adding to multiuser interference of the system as a whole and hence limiting its multiple-access capability. For a system with K users, each of whose signals arrive via M paths, we have a situation similar to a system with KM users transmitting along independent fading links similar to those considered above. Turin [8] shows that there is a five- to twentyfold decrease in the number of simultaneous users permissible in going from single-path nonfading links to dense, urban multipath links. This is caused by an aggravated version of the NFP, which arises from the fading of correlation noise, and its replication due to multipath propagation. In urban environments where several multipaths could arrive with similar energy but antiphase fading patterns, power control based on the primary received path is likely to enhance the interference component from an antiphase fading path. It follows that power control could prove to be self-defeating in a dense multipath environment.

C. The RAKE-SLWA Receiver

The RAKE receiver implementation in a DS-CDMA system exploits the concept of internal diversity, which is inherent to DS systems. Clearly the taps of the RAKE receiver [25], [26] are based on the CLCR and are hence prone to the NFP. Treating each multipath as an additional user in the system, decorrelating techniques can be applied to retrieve the significant multipaths. It is important to note that the problem of phase alignment, prior to combining the outputs of the individual RAKE receiver taps, is alleviated by using the differential scheme proposed earlier. Clearly, the dimension of the decorrelation problem is increased by a factor equivalent to the square of the number of multipaths being combined. A trade-off between complexity and performance will have to be arrived at in a practical system. As discussed in Section II-D, a decorrelating algorithm is probably the most inexpensive interference cancellation technique on a per-iteration (symbol) basis (also see Section IV, [10]). Significant linear system recomputation costs, however, impose a limit to multipath decorrelation. This will leave the system with residual multipath interference that will accumulate to limit capacity. Additional users will hence degrade the system by contributing to residual multipath interference. For a decorrelator with DPSK RAKE multipath combining, we have a decision variable D given by

$$D = \sum_{n=1}^{M} d_{k,n}(i) d^*_{k,n}(i-1) \tag{18}$$

where $d_{k,n}(i)$ is a complex decorrelator output for the nth path of the kth user over the ith symbol interval. We can write for B-DPSK

$$D = \sum_{n=1}^{M} d^I_{k,n}(i).d^I_{k,n}(i-1) + \sum_{n=1}^{M} d^J_{k,n}(i).d^J_{k,n}(i-1). \tag{19}$$

A schematic diagram of the resulting RAKE-SLWA receiver is shown in Fig. 8. The mobile radio channel simulation is based on a tapped delay line model [27]. In order to obtain realistic results in the light of excessive simulation time required for multiuser DS-CDMA, we assume an open-loop power control strategy that compensates for propagation loss and very slow fading. No compensation for fast fading is assumed. The tap weights for the channel model are independent Rayleigh distributed signals [27]. Doppler frequencies along each path of each user are derived from the vehicle speed and randomly assigned arrival angles. In light of equations (49), (60), (61) (see Section IV), the total interference variance is clearly dependent on three factors: a) magnitude of crosscorrelations (hence elements of $\mathcal{D}$, $\mathcal{M}$) determined by the SF, b) absolute dimension of the zero forcing problem, and c) magnitude of the residual multipath energy relative to the signal energy. The trade-off between the last two factors will depend largely on the delay profile of the channel. In terms of RAKE decorrelation, decorrelating additional paths reduces c) but increases b). Similarly, increasing SF for a fixed number of RAKE taps tends to decrease a) while increasing c). It is clear that adding users contributes to both b) and c). The effect of system parameters is sumamrized in Table I. The comparison

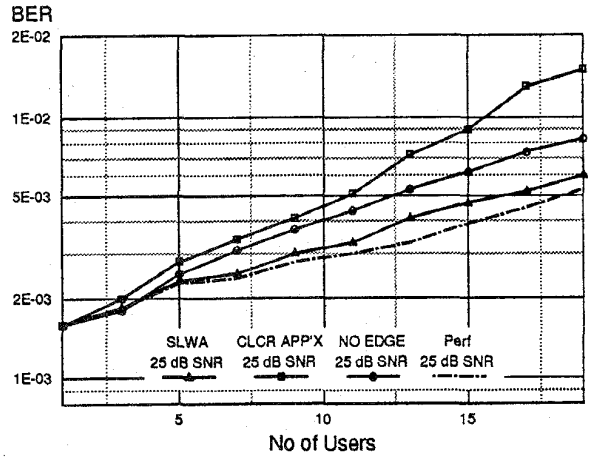

Fig. 10. Impact of edge correction—single-path fading, SF 63 (simulated).

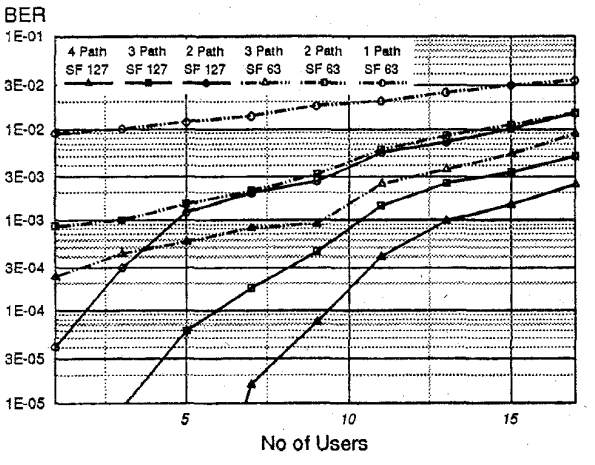

Fig. 12. Effect of SF and combining depth, 21.0 dB SNR (simulation).

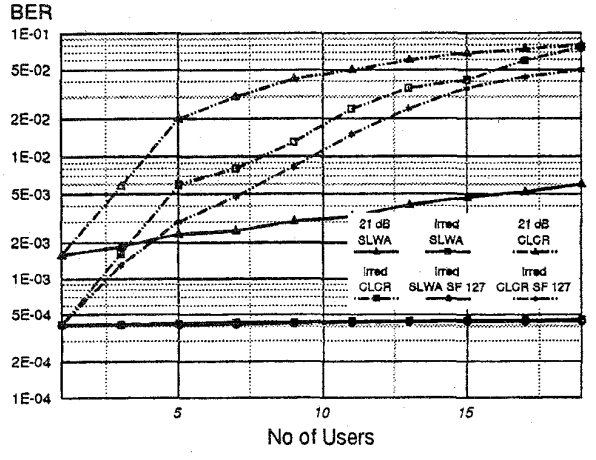

Fig. 11. Effect of combining depth, SF 127, 21.0 dB SNR (simulation).

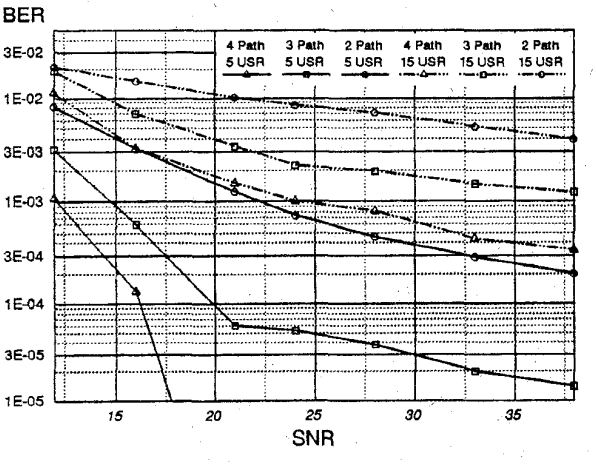

Fig. 13. Noise performance—SF 127 (simulation).

is made on the basis that the data rate remains constant, so that increasing the SF results in a proportional increase in the spread bandwidth. Fig. 11 clearly demonstrates the capacity improvements offered by increasing the combining depth in the case of the SLWA. In contrast, the CLCR performance is not improved once MA limited. Processing additional paths gives the decorrelator deterministic access to a larger proportion of the total multipath energy. As the combining depth is reduced, accumulated multipath energy affects the SLWA performance resulting in it eventually becoming MA-limited as well, and approaching the performance of the CLCR. It is seen from the analysis in [28] and from Fig. 12 (the simulation used an l-r sloping profile for the mean received path energies, with $T_m = 3.2\ \mu s$), that the lower correlation values result in the impact of c) being reduced at the higher SF. The benefits of combining additional paths is hence reduced as the SF is increased. Alternatively, the benefit (if any) of increasing the SF decreases as the number of combined paths is increased. In the limit, this suggests that single-path decorrelation will suffice for high SF (wideband) DS-CDMA. Fig. 12 also shows that bandwidth-efficient capacity improvements due to doubling the SF can be achieved only for moderate loading. The region over which such capacity improvements are available decreases as the combining depth is increased. Fig. 13 shows the SNR performance for selected numbers of users and combined paths.

IV. Decorrelator Filter Coefficient Updating Algorithm

Here we propose a novel algorithm for the dynamic updating of decorrelator coefficients, which lends itself to fully parallel ASIC implementation, thus making finite sequence length decorrelation comparable to successive cancellation techniques such as CDMA-IC [13] and minimum mean squared error (MMSE) techniques [29] in complexity. The decorrelator has a low per-iteration cost due to its standard zero-forcing operation. In contrast, CDMA-IC [13] is inherently a serial solution based on successive cancellation of users proposed by Viterbi [12]. A channel gain table needs to be maintained and updated in response to the dynamic nature of the mobile radio channel. Additional users or multipath combining hence represent additional steps in a serial process. MMSE algorithms for interference rejection make modest demands on information regarding interfering users. The frequency of

TABLE II
SUMMARIZED OPERATION COUNTS FOR FULL PARALLELISM

Task Performed	*Operation Count*	
	M, A	S,D
Single Row	$2K+1$	1
Full Matrix	$2K(2N-1)+2N$	$2N$
W/O Delay Ord	$2K(3N-2)+2N$	$2N$
Matrix Inv	$2K^2(N+1)+NK$	NK
Sync Correc'n	$2K+2$	2
Sync Matrix Inv	K^2+K	K

training required and adaptation strategies, which are critical factors for the dynamically varying mobile radio channel, have not been addressed fully in the literature. A bulk of the processing once again translates to a per-iteration processing load.

A. Finite Sequence Length Decorrelation

Central to the implementation a decorrelating algorithm is the solution of the linear system (13). The solution can be disected into the inversion or LU decomposition of the system matrix, followed by the repeated solution of the system for different LHS (corrected matched filter output vectors in SLWA) vectors. The former operation needs to be performed on a relatively infrequent basis. The latter, however, has to conform to the processing delay restrictions of the system.

1) Zero-Force Equalizer Implementation: Iterations are implemented inexpensively using a simple zero-force equalizer structure (Fig. 14). The tap weights for the equalizer are derived from the inverse crosscorrelation matrix. From (13), it is clear that

$$\hat{\boldsymbol{W}}\boldsymbol{B}_k(i) = \mathfrak{R}^{-1}_{k,i}.\boldsymbol{X} \tag{20}$$

where $\mathfrak{R}^{-1}_{k,i}$ is the kth row within the ith block of the inverse of $\mathfrak{R}$. The decorrelator is the simplest interference cancellation technique to implement on a periteration basis. Furthermore, specialized high-speed ZF equalizer IC technology is readily available. Let K be the total number of paths/users being decorrelated, and let $\boldsymbol{M}$, $\boldsymbol{A}$, $\boldsymbol{S}$, $\boldsymbol{D}$ denote multiplications, additions, subtractions and divisions, respectively. The cost of a single decorrelation operation is given by

$$\boldsymbol{ZF}\ \textbf{Cost}: NK\boldsymbol{M} + NK\boldsymbol{A}. \tag{21}$$

Fig. 14 also depicts the requirement to update the decorrelator filter coefficients in response to changes in the crosscorrelation matrix. This involves updating the inverse correlation matrix and represents a significant computational overhead. This problem is addressed below.

2) Solution Using LU Decomposition: Using the LU decomposition approach (particularly amenable to block tridiagonal systems) has attractive features from the viewpoint of storage requirements and if restricted to serial processing [10], [18]. Extending Stone's recursive doubling algorithm [20] for tridiagonal matrices to give a parallel algorithm for the block tridiagonal case, we have verified that the parallelization of the process is worthwhile only if $N \gg K$ [10], and hence is not applicable to loading scenarios found in practice. We now propose a strategy that avoids recomputing the linear system.

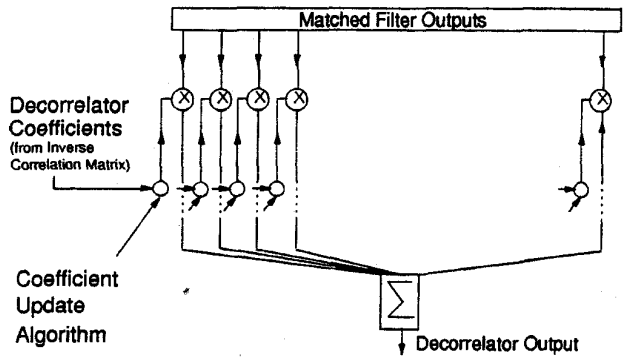

Fig. 14. Zero-forcing decorrelator.

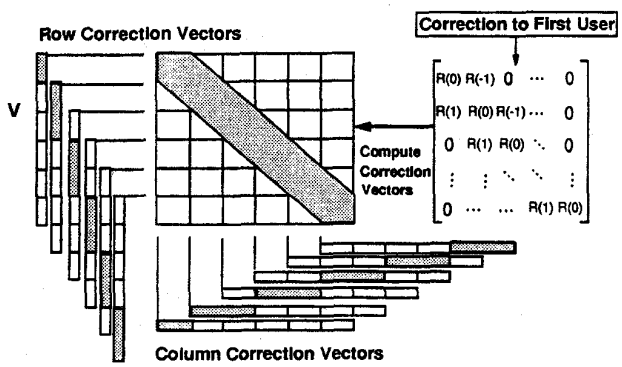

Fig. 15. Correction vectors—example.

B. Filter Coefficient Updating Algorithm

Here we propose a novel algorithm for updating the filter coefficients in response to changes in the correlation coefficients, using a fully parallel architecture. The architecture lends itself to a direct trade-off between parallelism and processing delay. The algorithm is based on the Sherman-Morrison Formula [31] and exploits the sparse nature of the block tridiagonal system matrix. We refer to Fig. 15 in the following discussion. A change with respect to one user or path will result in changes in the elements of a single row and column of the lower and upper triangular matrices $R(1)$ and $R(-1)$ and the symmetric matrix $R(0)$. It will only be in the worst case that all the cross-correlation coefficients related to the user concerned will change significantly. N rows and an equal number of columns need to be corrected. For clarity, we consider only row-wise corrections. Let $\boldsymbol{v}$, $\boldsymbol{u}$ be NK vectors. Let $\boldsymbol{v}$ be a row correction vector containing the corrections to the row of $\mathfrak{R}$ being considered. The sparsity of the vector $\boldsymbol{v}$ will depend on the number of coefficients affected. In the worst case, this vector will have only $2K$ (contiguous) nonzero elements (see Fig. 15). We note that

$$[\boldsymbol{u} \otimes \boldsymbol{v}]_{i,j} = \boldsymbol{u}[i].\boldsymbol{v}[j] \tag{22}$$

if $\boldsymbol{u}$ is the unit vector $\boldsymbol{e}_j$, then the correction vector can be applied (added) to the jth row of $\mathfrak{R}$ as follows:

$$\mathfrak{R} \rightarrow \mathfrak{R} + \boldsymbol{u} \otimes \boldsymbol{v}. \tag{23}$$

The new inverse matrix is then $(\mathfrak{R}+\boldsymbol{u}\otimes\boldsymbol{v})^{-1}$. Put $A = \boldsymbol{u}\otimes\boldsymbol{v}$

$$\begin{aligned}(\mathfrak{R}+A)^{-1} &= (I+\mathfrak{R}^{-1}A)^{-1}\mathfrak{R}^{-1} \\ &= \mathfrak{R}^{-1} - \mathfrak{R}^{-1}A\mathfrak{R}^{-1} + (\mathfrak{R}^{-1}A)^2\mathfrak{R}^{-1} \\ &\quad - (\mathfrak{R}^{-1}A)^3\mathfrak{R}^{-1} + \cdots \\ &= \mathfrak{R}^{-1} - (\mathfrak{R}^{-1}A\mathfrak{R}^{-1})(I - \mathfrak{R}^{-1}A + (\mathfrak{R}^{-1}A)^2 \\ &\quad - (\mathfrak{R}^{-1}A)^3 + \cdots). \end{aligned} \tag{24}$$

Expanding, replacing A by $\boldsymbol{u}\otimes\boldsymbol{v}$ and using the associativity of outer and inner products to factor out the scalar term $\beta = \boldsymbol{v}^T\mathfrak{R}^{-1}\boldsymbol{u}$

$$\begin{aligned}(\mathfrak{R}+\boldsymbol{u}\otimes\boldsymbol{v})^{-1} &= \mathfrak{R}^{-1} - \mathfrak{R}^{-1}.\boldsymbol{u} \\ &\quad \otimes\boldsymbol{v}.\mathfrak{R}^{-1}(1-\beta+\beta^2-\beta^3+\cdots). \end{aligned} \tag{25}$$

This leads to [17]

$$\mathfrak{R}^{-1} \rightarrow \mathfrak{R}^{-1} - \frac{z\otimes w}{1+\beta} \tag{26}$$

where

$$z = \mathfrak{R}^{-1}\boldsymbol{u} \qquad \boldsymbol{w} = (\mathfrak{R}^{-1})^T\boldsymbol{v} \qquad \beta = \boldsymbol{v}.z. \tag{27}$$

Without loss of generality, consider a correction initiated by the first user and the corresponding row in the second block of $\mathfrak{R}$. The edge blocks are special cases (even more sparse) [17]. $\boldsymbol{u}$ is in this case the $(K+1)^{st}$ unit vector, and $\boldsymbol{v}$ is all zero except for the first $2K$ elements. We require only one such correction vector, since the others are easily derived by a cyclic shift. Define $\mathcal{P}$ to be a sub-matrix of $\mathfrak{R}^{-1}$ of dimension $2K \times NK$ comprising the rows corresponding to the $2K$ nonzero elements of $\boldsymbol{v}$. Further denote the nonzero part of $\boldsymbol{v}$ by $\tilde{\boldsymbol{v}}$ and denote the xth column of a matrix M by M_x. Considering each of the terms given by (27) in turn, it can be shown that [17]

$$z = (\mathfrak{R}^{-1})_{K+1} \tag{28}$$

$$\boldsymbol{w} = \tilde{\boldsymbol{v}}^T\mathcal{P} \tag{29}$$

$$\beta = \boldsymbol{w}_{K+1}. \tag{30}$$

We have hence expressed the terms of (27) in terms of the rows and columns of the inverse system matrix $\mathfrak{R}^{-1}$ and the correction vector.

1) Estimation of Operation Counts: Here the computations involved in correcting the system matrix is estimated. $\boldsymbol{w}$ from (29) is given by

$$\boldsymbol{w}_j = \sum_{i=1}^{2K} \tilde{\boldsymbol{v}}_i.\mathcal{P}_j(i). \tag{31}$$

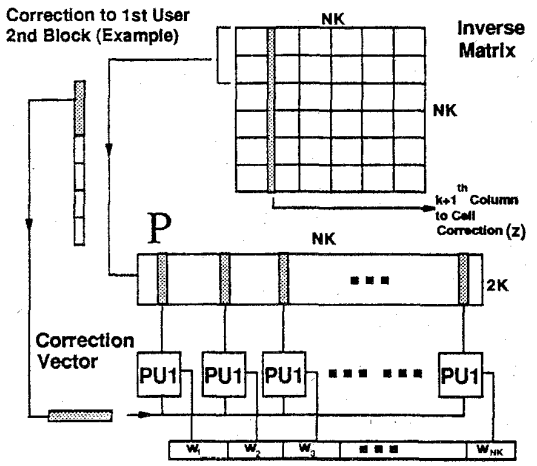

Fig. 16. Parallel correction setup.

Clearly, this is the overhead cost incurred for any one row or column correction. Let a processing unit PU1 perform an operation of the form

$$\sum_{j=1}^{2K} \tilde{\boldsymbol{v}}_j.\boldsymbol{p}_j$$

where $\boldsymbol{p}$ is a column of $\mathcal{P}$. By using NK degree parallelism at this stage (see Fig. 15), the serial operation count is $2K\boldsymbol{M} + 2K\boldsymbol{A}$ and can be implemented using multiply–accumulate devices. Now, let

$$Q = z \otimes \boldsymbol{w} \quad \text{giving}$$

$$Q_{i,j} = \mathfrak{R}^{-1}_{i,K+1}.\sum_{l=1}^{2K} \tilde{\boldsymbol{v}}_l\mathcal{P}_j(l). \tag{32}$$

Substituting in (26) from (28), (30), (32) we have

$$\mathfrak{R}^{-1}_{i,j} \rightarrow \mathfrak{R}^{-1}_{i,j} - \frac{Q_{i,j}}{1+\boldsymbol{w}_{K+1}}. \tag{33}$$

The single-cell correction operation count is hence $1\boldsymbol{M} + 1\boldsymbol{A} + 1\boldsymbol{S} + 1\boldsymbol{D}$. Varying degrees of parallelism can be used at this stage, depending on ergonomic restrictions, cost, and state-of-the-art ASIC technology. We note that there is no specific need to locate all cells performing (33) on the same device. Full parallelism is hence feasible by dividing up the row or column space over several identical IC's. Configurations for reduced parallelism and corresponding operation counts are found in [17]. Clearly, we have to repeat the operation discussed above $2N$ times, taking into account the edge blocks.

The correction algorithm is given below for the fully parallel cell computation. When an interval of the form $[1 \le j \le N]$ appears after a statement, that statement is assumed to be executed simultaneously for all indices in that interval. The

mathematical expression being executed is enclosed in $\{.\}$. We assume the correction applies to the kth user.

Correction Algorithm:

BEGIN
Setup row (v), column (u) correction vectors
FOR x = rows (r), columns (c) DO
  Setup $\tilde{v}$ $\tilde{u}$ from r (c) correction vectors
    FOR (i = 1 STEP i, UNTIL N)
      IF (i NEQ 1) AND (i NEQ N)
        Set P to $2K$ rows of $\mathfrak{R}^{-1}$
          start : $((i-2)K+k)^{th} \times (r/c)$
      ELSE
        IF (i EQ 1)
          Set P to $(K+k-1) \times (r/c)$'s of $\mathfrak{R}^{-1}$
            start : $((i-1)K+k)^{th} \times (r/c)$
        ELSE
          Set P to $(2K-k) \times (r/c)$'s of $\mathfrak{R}^{-1}$
            start : $((i-1)K+k)^{th} \times (r/c)$
      Set z to $((i-1)K+k)^{th}$, $\overline{x}(c/r)$
      Compute w_j; $[1 \le j \le NK]\left\{\sum_{j=1}^{2K} \tilde{v}_j.p_j\right\}$
      Compute $Q_{p,q}$; $[1 \le p, q \le NK]\{z_p.w_q\}$
      Compute Correction $\Delta_{p,q}$; $[1 \le p, q \le NK]\frac{Q_{p,q}}{1+W_{(i-1)K+k}}$;
      Apply Correction to $\mathfrak{R}_{p,q}^{-1}$; $[1 \le p, q \le NK]\mathfrak{R}_{p,q}^{-1} \rightarrow \mathfrak{R}_{p,q}^{-1} - \Delta_{p,q}$
END

The upper/lower triangular structure of the matrices $R(-1)$, $R(1)$ relies on the users being ordered according to their delays. Clearly, the condition ceases to hold if the timing of a user changes to such an extent as to change its position in the delay table, requiring repeated swapping of users. From this point of view, it is beneficial in the long term to remove the restriction on delay-ordering. $\mathfrak{R}$ remains block tridiagonal, but $R(-1)$ and $R(1)$ have to be treated as being full matrices. We hence have a contiguous block of $3K$ potentially nonzero elements in the correction vectors. A moderate number of new users can be accommodated by maintaining unused slots in the correlation matrices and correcting them to accommodate the new user. An attractive feature of the strategy is that, once in place, the hardware architecture can be used to compute the matrix inverse in the first instance or periodically thereafter. We start with $\mathfrak{R} = \mathfrak{R}^{-1} = I$. NK row corrections are applied to $\mathfrak{R}$ so as to arrive at the desired partial correlation matrix.

2) Synchronous DS-CDMA: In the case of synchronous DS-CDMA, the algorithm collapses to the original Sherman-Morrison formula. Clearly, only $R(0)$ exists, and hence only one row operation and one column operation are required. The correction vectors are now full but have only K elements. K degree parallelism can be used to compute $\boldsymbol{w}$. $\boldsymbol{z}$ is a column of $R(0)$, and (26)–(30) and (33) hold as before. The cell computations can be performed fully in parallel with only K^2 processing units. The architecture can be extended as before to compute the matrix inverse. The operation counts are summarized in Table I.

V. Mathematical Analysis of Sliding Window Decorrelator

Here we summarize the development of a mathematical model for the sliding window decorrelator operating in a multiuser asynchronous, differentially coherent DS-CDMA system. The exact BER analysis of the sliding window receiver is not analytically tractable due to the edge-correction involved. We hence make the simplifying assumption that perfect edge correction is achieved. The accuracy of this assumption increases as the overall error rate decreases, as seen from Figs. 9 and 10. The standard decorrelator [1] has been analyzed in [32] and [33] for a quasi-stationary channel assuming optimum (complete) RAKE combining. In addition to the analysis of a sliding window system, the contribution of this work is the analysis for a nonstationary channel and the effects of incomplete RAKE decorrelation/combining. The model can be used to investigate the effects of RAKE combining depth, spreading factor and code sets, symbol rate, and window size on the performance of the receiver in AWGN, single-path and multipath fading channels. The analysis is for differential BPSK.

A. Terminology

We consider a K user system. E_j, A_j are the received energy and amplitude respectively, of the jth user, whose relative delay is denoted by τ_j. θ_j is the carrier phase of the jth user incorporating the transmit data polarity during the current symbol interval. For the analysis in fading, let $g_j(t)$ and ϕ_j be the amplitude and phase variations due to fading, respectively, for the jth user. More terminology is introduced as the analysis progresses and unless otherwise specified corresponds to that in Section II.

B. Differential Detection in AWGN

Let the statistics obtained over adjacent symbol intervals be X and Y. Our decision variable is then a special case of the Gaussian quadratic form and is given by $D = XY^* + X^*Y$. The probability of error can be derived in terms of the means $\overline{X}$ and $\overline{Y}$, and the second central moments M_{xx}, M_{yy}, and M_{xy}. Without loss of generality, we consider the first user, when users are numbered according to their delays. Further, no generality is lost by setting the relative delay of this user to zero. We denote the matched filter outputs in adjacent symbol intervals as $y_1(i)$ and $y_1(i-1)$

$$y_1(i) = \sum_{j=1}^{K} E_j^{\frac{1}{2}} \{\exp[j\theta_{j,i-1}]R_{1,j}(1) + \exp[j\theta_{j,i}]R_{1,j}(0)\} + n_1(i) \quad (34)$$

where

$$n_1(i) = \int_{iT}^{(i+1)T} n(t-iT).\tilde{s}_1(t-iT)\,dt.$$

We denote the decorrelating detector for the ith bit of our (jth) user by $\boldsymbol{h}_{i,j}$. The detector is defined to be the jth row within the ith block of the inverse matrix $\mathfrak{R}^{-1}$. Let the window span be W bits, and assume the window slides by one vector each iteration providing W estimates for averaging. From the properties established in [1], the decorrelator outputs are void of multiuser interference terms giving

$$X = E_1^{\frac{1}{2}} \exp(j\theta_{1,pi}) + \frac{1}{W}\sum_{l=p+1}^{i}\sum_{j=0}^{W-1}\sum_{k=1}^{K} \boldsymbol{h}_{l-p}^{jK+k}.\boldsymbol{n}_{l,j}^{k}$$

$$Y = E_1^{\frac{1}{2}} \exp(j\theta_{1,i-1}) + \frac{1}{W}\sum_{l=p}^{i-1}\sum_{j=0}^{W-1}\sum_{k=1}^{K} \boldsymbol{h}_{l-p+1}^{jK+k}.\boldsymbol{n}_{l,j}^{k} \quad (35)$$

where

$$\boldsymbol{n}_{i,j}^{k} = \int_{(i+j)T+\tau_k}^{(i+j+1)T+\tau_k} n(t-(i+j)T-\tau_k) \cdot\tilde{s}_k(t-(i+j)T-\tau_k)\,dt \quad (36)$$

and $p = i - W$, denotes the starting point of the window under consideration. The summations on the right-hand side of (35) are zero mean Gaussian random variables with identical variance ($M_{xx} = M_{yy}$). For differentially encoded transmission of $+1$, we have $\overline{X} = \overline{Y} = E_1^{1/2}$.

1) Evaluation of Second Central Moments: The noise correlation term μ_n can be written using a set of noise covariance matrices $\mathcal{D}(i)$, where i represents the lag between the data windows being correlated. Let the start positions of the windows being correlated by q and r and the corresponding data items being detected be s and t, where $q - r = s - t$. A typical correlation term can be written [28]

$$\mu_n = \boldsymbol{h}_s^T \mathcal{D}(q-r)\boldsymbol{h}_t.2\sigma^2. \quad (37)$$

Details of the evaluation of the noise covariance matrix can be found in [1] and [28]. It can be shown that

$$\mathcal{D}_{(jK+k),(mK+n)}(i) = \begin{cases} R_{k,n}(0) & \text{if } m-j=i \text{ and } \tau_k = \tau_n \\ 0 & \text{otherwise} \end{cases} \quad (38)$$

where $0 \le j, m \le W-1$ and $1 \le k, n \le K$. In the case of M_{xy}, we must introduce the effect of correlating over adjacent symbol intervals

$$\tilde{\mu}_n = \boldsymbol{h}^T \mathcal{D}(q-r+1)\boldsymbol{h}.\sigma^2. \quad (39)$$

We now return to the problem of evaluating M_{xx}, M_{yy}, and M_{xy}. From equations (35), (37), and (39)

$$M_{xx} = \frac{2}{W^2}\sum_{i=1}^{W}\sum_{j=1}^{W} \boldsymbol{h}_{(W-i)}^T \mathcal{D}(i-j)\boldsymbol{h}_{(W-j)}\sigma^2 \quad (40)$$

$$M_{xy} = \frac{2}{W^2}\sum_{i=1}^{W}\sum_{j=1}^{W} \boldsymbol{h}_{(W-i)}^T \mathcal{D}(i-j+1)\boldsymbol{h}_{(W-j)}\sigma^2. \quad (41)$$

Using the expression for the probability of error in the case of B-DPSK based on the Gaussian quadratic form [25], it is shown in [28] that for the case under considerations, the probability of error can be written in terms of the SNR per bit γ

$$P_1^d(\gamma) = \left(1 - \frac{M_{xx} - M_{xy}}{2M_{xx}}\right) \cdot\exp\left(-\frac{\gamma.W^2}{\left[\sum_{i=1}^{W}\sum_{j=1}^{W} \boldsymbol{h}_i^T \mathcal{D}(i-j)\boldsymbol{h}_j\right]}\right). \quad (42)$$

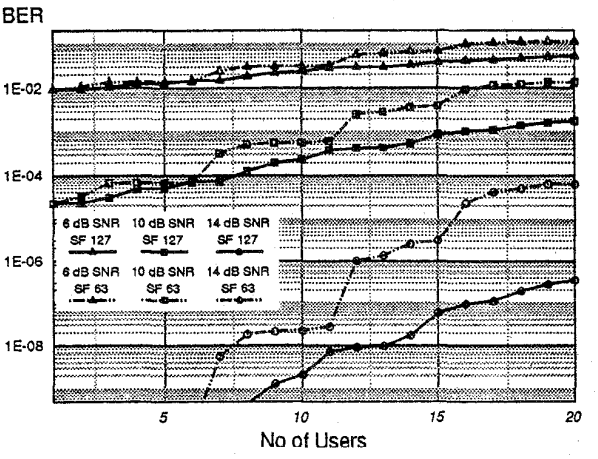

Fig. 17. Effect of SF for fixed SNR (AWGN, numerical).

Figs. 17 and 18 are numerical examples obtained from the analytical model described. From Fig. 17 it is clear that the impact of thermal noise is more significant than that of the number of users, as would be expected from a decorrelating solution. Both graphs show that the impact of SF increases as the number of users is increased. This arises because of the growing size of the decorrelation problem and the higher level of interference enhancement at the lower SF. The results also demonstrate that the SF has less significance as the channel gets noise limited. Fig. 19 shows the deterioration in performance as the number of users approaches the processing gain (PG) of the system. It is seen that interference enhancement effects preclude the use of decorrelation to achieve bandwidth-efficient multiple access in large systems at standard operating SNR's.

C. Performance Analysis in Multipath Fading Channels

Consider a time-variant frequency-selective channel over which direct sequence signaling is employed. Let the total multipath spread be T_m and the chip period and symbol period be T_c and T_s, respectively. We assume that $T_s \gg T_m$, thereby neglecting any intersymbol interference due to multipath. With reference to equation (17), the magnitudes $|c_n(t)| = g_n(t)$ are assumed Rayleigh distributed and their phases $\phi_n(t)$ uniformly distributed on $(2\pi]$, with independence between taps from the uncorrelated scattering assumption [25]. The decision variable for the RAKE decorrelator Fig. 8 is given by

$$D = \sum_{k=1}^{M} X_k Y_k^* + X_k^* Y_k = \sum_{k=1}^{M} d_k \quad (43)$$

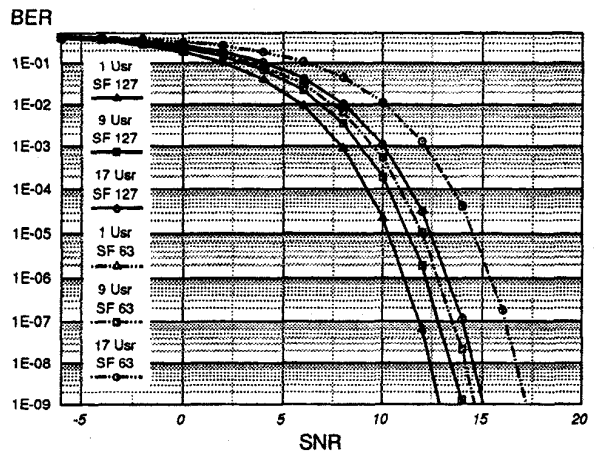

Fig. 18. Effect of SF for fixed loading (AWGN, numerical).

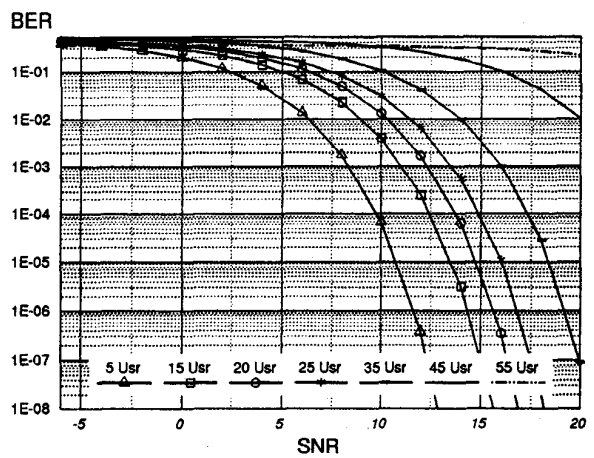

Fig. 19. Bandwidth-efficient system in AWGN, SF 63 (numerical).

where X_k and Y_k are the outputs from the kth decorrelated RAKE tap during consecutive symbol intervals. We collect the decision statistics into a vector $\boldsymbol{w}$

$$\boldsymbol{w} = \begin{bmatrix} \boldsymbol{w}_X \\ \boldsymbol{w}_Y \end{bmatrix} \tag{44}$$

where $\boldsymbol{w}_X^T = [X_1, \cdots, X_M]$ and similarly for $\boldsymbol{w}_Y$. The decision statistic can be written as a Hermitian quadratic form [33], [34], [35]

$$D = \boldsymbol{w}^T Q \boldsymbol{w} \tag{45}$$

For the case of differentially coherent detection, we have

$$Q = \begin{pmatrix} 0 & 0.5\boldsymbol{I}_M \\ 0.5\boldsymbol{I}_M & 0 \end{pmatrix}. \tag{46}$$

An expression for the probability of error is derived in [28] in terms of the eigenvalues λ_i of the matrix $R_{ww} = W.Q$

$$P_e = \sum\nolimits_{i,\lambda_i<0} \Gamma_i \quad \text{where} \quad \Gamma i = \prod_{\substack{i=1 \\ k\neq i}}^{2M} \frac{\lambda_i}{\lambda_i - \lambda_k}. \tag{47}$$

W is the covariance matrix of the decision vector $\boldsymbol{w}$. We partition the covariance matrix W

$$W = \begin{pmatrix} W_{11} & W_{12} \\ W_{12}^T & W_{22} \end{pmatrix}. \tag{48}$$

The users are assumed ordered according to their delays, and the paths of each user are grouped together. The partial correlation matrices now have dimension $SK \times SK$, and the arrangement of the elements differs from that defined earlier in that the crosscorrelation terms pertaining to paths of the same user are grouped together. We define a set of residual crosscorrelation matrices $P(i)$ having dimension $MK \times K(S-M)$. The entries are the partial correlation coefficients between each of the MK decorrelated paths and the $(S-M)K$ paths that are not resolved by the RAKE receiver. We define the following notation

$$P_{i:p,j;q}(l) \equiv P_{M(i-1)+p),((S-M)(j-1)+(q-M))}(l).$$

We can now write the quadrature matched filter output for the kth path of the jth user during the λ th symbol interval. For clarity, we analyze (with no loss of generality—due to the independence of terms on quadrature branches) only one of the quadrature terms

$$y_{j,k}^I(t - \lambda T) = \alpha_{j,k}(\lambda) + \beta_{j,k}(\lambda) + \eta_{j,k}(\lambda). \tag{49}$$

The decorrelating detector for the ith bit within a particular window for the yth path of the xth user is denoted by $\boldsymbol{h}_{y,i}$. For the purpose of analysis, stationarity of phase is assumed over the sliding span of the decorrelating window. We have for the multipath case

$$d_y^I(i) = \frac{1}{W} \sum_{l=p+1}^{i} \sum_{h=0}^{W-1} \sum_{j=1}^{K} \sum_{k=1}^{M} \boldsymbol{h}_{y,l-p}^{hMK+M(j-1)+k} . y_{j,k}^I(l+h) \tag{50}$$

where $p = i - W$. Referring back to (49), $\alpha_{j,k}(\lambda)$ represents the contribution of the MK paths to be decorrelated. It is clear from the properties of the decorrelating detector [1] that these terms are eliminated except when $(j, k, i) = (x, y, z)$, in which case we are left with the desired signal. This leaves us with an interference term, which is a function of the correlated thermal noise $\eta_{j,k}(i)$ and the residual interference $\beta_{j,k}(i)$, which is made up of contributions from each of the $(S-M) \times K$ paths outside the decorrelation and combining depth. The residual interference term is given by

$$\beta_{j,k}(\lambda) = \sum_{p=1}^{K} A_p [b_p^{\lambda-1} \xi_p^{j,k}(1;\lambda) + b_p^{\lambda} \xi_p^{j,k}(0;\lambda) + b_p^{\lambda+1} \xi_p^{j,k}(-1;\lambda)]. \tag{51}$$

The noise samples $\eta_{j,k}(\lambda)$ are independent zero mean Gaussian random variables with identical variance $\sigma^2 (= N_0 T)$. The residual interference term is expanded in [28]. The $\xi_p^{j,k}(i;\lambda)$ terms represent the residual interference contribution from the pth user to the j, kth matched filter output and are of the form

$$\xi_p^{j,k}(i;\lambda) = \sum_{q=M+1}^{S} P_{j,k;p,q}(i) \cdot \int_{\tau_{j,k}}^{\tau_{p,q}} g_{p,q}(t - (\lambda - i)T - \tau_{p,q}) . \cos(\phi_{p,q}). \tag{52}$$

We aim at developing a model parameterized on a particular system configuration since a general result requires a degree of Monte Carlo simulation [36]. It can be shown [28] that the random variables $\xi_p^{j,k}(i;\lambda)$, $(i=-1, 0, 1)$, for all p, λ are zero mean Gaussian random variables and that

$$E[\beta_{j,k}(\lambda).\beta^*_{m,n}(\varphi)] = 0 \text{ if } |\varphi-\lambda|>1. \tag{53}$$

The decision variables for the x, yth path can be written

$$\begin{aligned} X_y &= A_x b_x^z . \int_{zT+\tau_{x,y}}^{(z+1)T+\tau_{x,y}} g_{x,y}(t-zT-t_{x,y})\,dt.\cos(\phi_{x,y}) \\ &\quad + \frac{1}{W}\sum_{l=p+1}^{z}\sum_{h=0}^{W-1}\sum_{j=1}^{K}\sum_{k=1}^{M} \boldsymbol{h}_{y,l-p}^{hMK+M(j-1)+k} \\ &\quad \cdot [\eta_{l,h}^{M(j-1)+k} + \beta_{j,k}(l+h)] \\ &\quad + \jmath . A_x b_x^z . \int_{zT+\tau_{x,y}}^{(z+1)T+\tau_{x,y}} \\ &\quad \cdot g_{x,y}(t-zT-\tau_{x,y})\,dt.\sin(\phi_{x,y}) \\ &\quad + \jmath . \frac{1}{W}\sum_{l=p+1}^{z}\sum_{h=0}^{W-1}\sum_{j=1}^{K}\sum_{k=1}^{M} \boldsymbol{h}_{y,l-p}^{hMK+M(j-1)+k} \\ &\quad \cdot [\nu_{l,h}^{M(j-1)+k} + \tilde{\beta}_{j,k}(l+h)] \end{aligned} \tag{54}$$

and similarly for Y_y, where $p=z-W$ and the notation for the noise samples has changed such that $\eta_{l,h}^{M(j-1)+k} \Leftrightarrow \eta_{j,k}(l+h)$. The random variables X_y and Y_y have zero mean for the Rayleigh fading case [28]. For the purposes of evaluating the submatrices $W_{i,j}$, we define three sets of matrices $\mathcal{M}^{11}$, $\mathcal{M}^{22}$, and $\mathcal{M}^{12}$. The matrices have dimension $NMK \times NMK$ and the abbreviated notation

$$\begin{aligned} &\mathcal{M}_{l;m;n.i;j;k} \equiv \\ &\quad \mathcal{M}_{MK(l-1)+M(m-1)+n,MK(i-1)+M(j-1)+k} \\ &\mathcal{M}^{11}_{l;m;n,i;j;k}(r,s) = \frac{1}{2N_0T}E[\beta_{j,k}(r+i).\beta^*_{m,n}(s+l)] \end{aligned} \tag{55}$$

$$\mathcal{M}^{22}_{l;m;n,i;j;k}(r,s) = \frac{1}{2N_0T}E[\beta_{j,k}(r+i-1).\beta^*_{m,n}(s+l-1)] \tag{56}$$

$$\mathcal{M}^{12}_{l;m;n,i;j;k}(r,s) = \frac{1}{2N_0T}E[\beta_{j,k}(r+i).\beta^*_{m,n}(s+l-1)]. \tag{57}$$

is used. The noise covariance matrix $\mathcal{D}$ of (38) can be rewritten for the multipath case as

$$\begin{aligned} &\mathcal{D}_{jMK+hM+k),(lMK+mM+n)}(i) \\ &\quad = \begin{cases} R_{h,k;m.n}(0) & \text{if } l-j=i \text{ and } \tau_{h,k}=\tau_{m,n} \\ 0 & \text{otherwise} \end{cases} \end{aligned} \tag{58}$$

where $0 \le j, l \le W-1$, and $0 \le h, m \le K-1$ and $1 \le k, n \le M$. From the independence of the quadrature

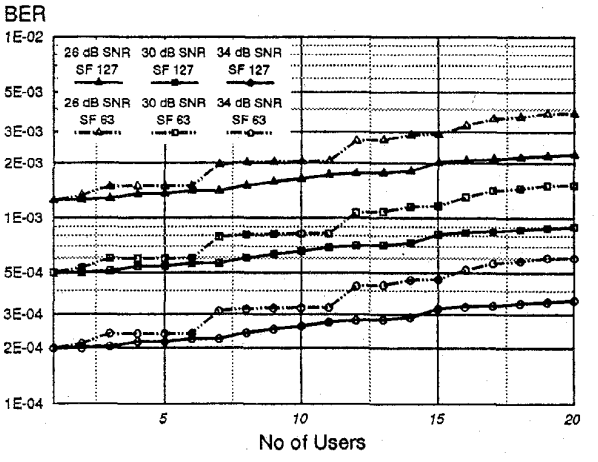

Fig. 20. Effect of SF for fixed SNR (single-path fading, numerical).

expectation terms we have, for the submatrices in (48)

$$\begin{aligned} &W_{e,f}(p,q) \\ &= \Sigma_{p,q}\mu_g^{x,p}((f-e)T) \\ &\quad + \frac{1}{W^2}\sum_{i=1}^{W}\sum_{j=1}^{W} \boldsymbol{h}^T_{p,W-i}.\mathcal{M}^{e,f}(i,j).\boldsymbol{h}_{q,W-j} \\ &\quad + \frac{1}{W^2}\sum_{i=1}^{W}\sum_{j=1}^{W} \boldsymbol{h}^T_{p,W-i}\mathcal{D}(i-j+(f-e))\boldsymbol{h}_{q,W-j} \end{aligned} \tag{59}$$

where Σ is the covariance matrix of the single user fadin channel and $\mu_g^{u,v}$ is the fading correlation coefficient of the vth path of the uth user. The fading correlation coefficient is related to the vehicle speed and hence the Doppler frequency by (for the jth path of the desired user) [37]

$$\mu_g = \frac{R_g^j(\tau)}{R_g^j(0)} = J_0(2\pi f_D^j \tau)$$

where $R_g^j(\tau) = E[g_j(t)g_j^*(t-\tau)]$ and J_0, is the zeroth-order Bessel function of the first kind. In our case of independent fading, Σ is a diagonal matrix with $\Sigma_{pp} = \gamma_{x,p}$. The error probability follows from evaluating the eigenvalues of the matrix $W.Q$ and equation (47). We consider single-path fading (typical of a suburban environment). The numerical results of Fig. 20 support the simulation results of Figs. 6 and 7. In Fig. 21 the effect of SF is more significant for a larger number of users because of the increased magnitude of the decorrelation problem. Fig. 22 shows the deterioration in performance as the number of users approaches the PG. So far, we have considered an exact computation of the intererence covariance matrices, the setting up of which is computationally expensive for the multipath case. We now consider a simpler approach that makes use of the Gaussian approximation for multiuser interference [36].

1) Multipath Fading Analysis Using Gaussian Approximation: With reference to the exact analysis, the terms $\alpha_{j,k}(\lambda)$, $\beta_{j,k}(\lambda)$, of (49) and (51) are assumed to be complex Gaussian.

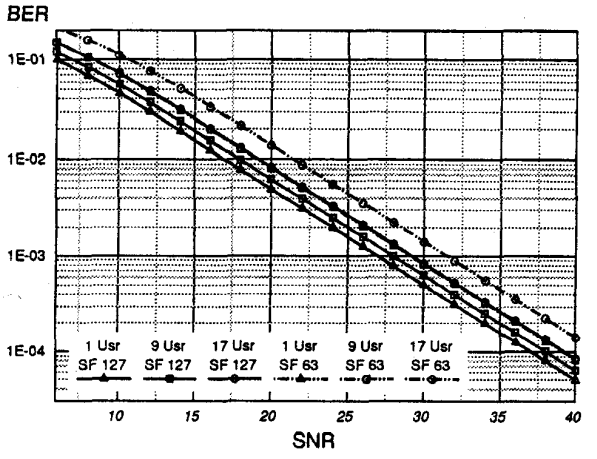

Fig. 21. Effect of SF for fixed loading (single-path fading, numerical).

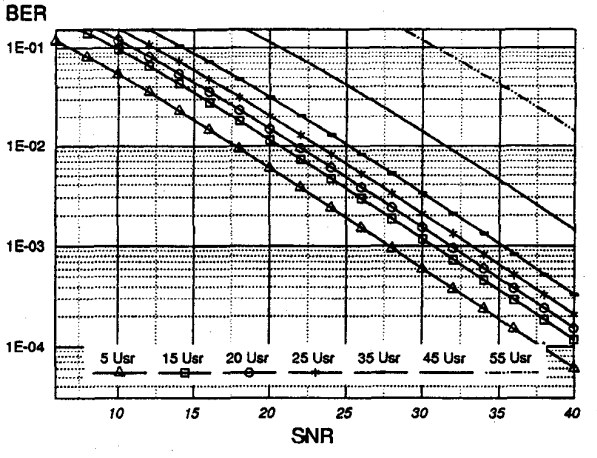

Fig. 22. Bandwidth-efficient system in single-path fading, SF 63 (numerical).

The accuracy of this assumption is discussed in [38]. We define the single random variable $\Delta_{j,k}(\lambda) = \Delta^I_{j,k}(\lambda) + \jmath.\Delta^J_{j,k}(\lambda)$, once again considering only one of the quadrature branches

$$\Delta^I_{j,k}(\lambda) = \beta_{j,k}(\lambda) + \eta_{j,k}(\lambda). \tag{60}$$

The results of [36] and [39] are extended in [28] for the case of unequal fading power on individual paths. $\Delta^I_{j,k}$ is, in fact, a summation of $(S - M)K$ random variables (interferers) $\chi^{\lambda}_{p,q}$ where

$$\chi^{\lambda}_{p,q} = b_p^{\lambda-1}\xi_p^{j,k}(1:\lambda)_q + b_p^{\lambda}\xi_p^{j,k}(0;\lambda)_q + b_p^{\lambda+1}\xi_p^{j,k}(-1;\lambda)_q$$

and $\xi_p^{j,k}(i;\lambda)_q$ denotes the qth term in the summation of equation (52). We then have

$$E[|\Delta_{j,k}(\lambda)|^2] = 2\left(N_0T + \sum_{p=1}^{K}\sum_{q=M+1}^{S} A_p^2T^2R_g^{p,q}(0)\epsilon^2\right). \tag{61}$$

ϵ^2 is shown to be equal to $\frac{2}{3N_c}$ [38], where N_c is the spreading factor. We can then write [28]

$$E[|\Delta_{j,k}(\lambda)|^2] = 2N_0T + \psi_{11}^{j,k} \tag{62}$$

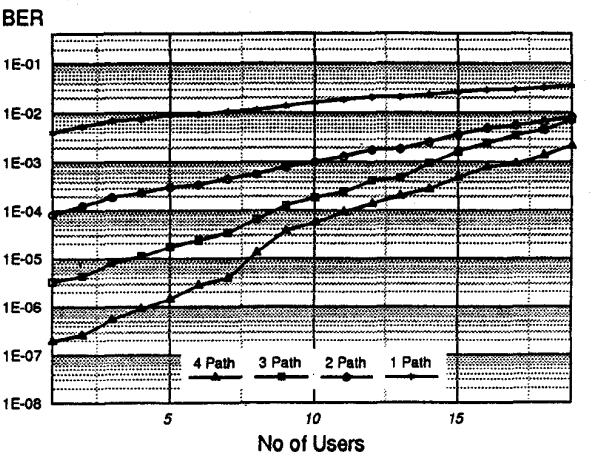

Fig. 23. Effect of combining depth at 22 dB (numerical).

where

$$\psi_{11}^{j,k} = \frac{4}{3N_c}\sum_{p=1}^{K}\sum_{q=M+1}^{S}\gamma_{p,q}. \tag{63}$$

Furthermore, as justified in [28] for an asynchronous system, we can write

$$E[\Delta_{j,k}(\lambda).\Delta_{p,q}(\varphi)^*] = 0 \quad \text{if} \quad \varphi \neq \lambda \quad \text{and} \quad (j,\,k) \neq (p,\,q). \tag{64}$$

The matrices of (55)–(57) can be written (clearly $\mathcal{M}^{11} = \mathcal{M}^{22}$)

$$\mathcal{M}^{11}_{l;m;n,i;j;k} \cdot (r,\,s) = \begin{cases} \psi_{11}^{j,k} & \text{for } r - s = l - i, \text{ and } (m,n) = (j,k) \\ 0 & \text{otherwise} \end{cases} \tag{65}$$

$$\mathcal{M}^{12}_{l;m;n,i;j;k} \cdot (r,\,s) = \begin{cases} \psi_{11}^{j,k} & \text{for } r - s = l - i + 1, \text{ and } (m,n) = (j,k) \\ 0 & \text{otherwise.} \end{cases} \tag{66}$$

The matrices W_{ij} are derived as before. The numerical results of Figs. 23 and 24 are for an SF of 127. The numerical curves support the trends of the simulation results of Figs. 11–13. Comparing Figs. 13 and 24, the crossover between the various combining depths is seen to be approached at a lower SNR in the case of the simulated (nonideal) case. From Fig. 23 it is clear that the potential benefit from combining additional paths in the case of an l-r sloping power delay profile decreases as the number of users and the magnitude of the problem increases. The idealized analysis shows superior performance over the simulated case, due both to the assumptions made and to the fact that instantaneous NF effects caused by fast fading are not fully accounted for in a mathematical analysis.

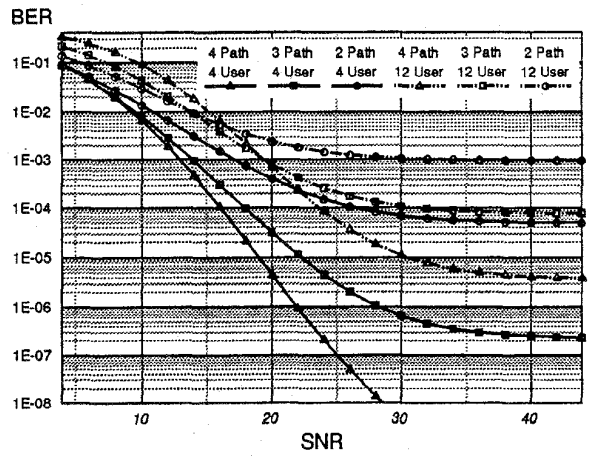

Fig. 24. Effect of users and combining depth (numerical).

VI. Conclusion

In this paper we have proposed a sliding window decorrelating algorithm, which when combined with RAKE multipath combining offers large capacity improvements over the CLCR in a mobile radio environment. The algorithm is based on a finite sequence length formulation and is hence less complex and more flexible than the standard decorrelator. A mathematical model that investigates in particular the impact of residual multipath energy was developed. Numerical results, together with those from simulation, where presented.

The algorithm is seen to ameliorate the requirement for closed-loop power control if sufficient diversity is used for a given combining depth. The CLCR, however, is rendered unusable by multipath fading in the absence of dynamic power control. An interplay between system parameters, such as combining depth, loading, SF, and PN code correlation properties, was identified and discussed. The results have shown that it is possible, by increasing the SF, to reduce the combining depth required in the case of channels with decaying power delay profiles, which are often encountered in practice. These findings augur well for the application of decorrelation for wider BW's. In the limit, this should allow primary (single path) decorrelation for wideband CDMA. In a practical system, however, bandwidth efficiency and complexity issues are important. It was seen from the results that under such constraints a decorrelating solution is likely to be positioned for low- to medium-spread bandwidths where the dual benefits of low residual energy for a given combining depth and low interference enhancement can be achieved.

We have also addressed some of the complexity issues of finite sequence length decorrelation. Competing solutions to the decorrelator have significantly larger per-iteration cost. The computational overhead of the decorrelator lies in the recomputation of the linear system solution on an infrequent basis. To alleviate this problem, we have proposed a coefficient correction algorithm for finite sequence length decorrelators. The algorithm is suitable for implementation on a fully parallel ASIC.

We can hence conclude that the large capacity improvements offered by the SLWA over the CLCR, low periteration cost, and the potential solution to the recomputation problem proposed make the SLWA an attractive centralized solution to the near–far problem.

References

[1] R. Lupas and S. Verdu, "Near–far resistance of multi-user detectors in asynchronous channels," *IEEE Trans. Commun.*, vol. 38, pp. 496–508, Apr. 1990.

[2] A. Salmasi and K. Gilhousen, "On the system aspects of code division multiple access (CDMA) applied to digital cellular and personal communications networks," in *41st IEEE Veh. Technol. Conf.*, St. Louis, MO, May 1991, pp. 57–62.

[3] G. Turin, F. Clapp, T. Johnston, S. Fine, and D. Lavry, "A statistical model of urban multi-path propagation," *IEEE Trans. Veh. Technol.*, vol. VT-21, pp. 1–9, Feb. 1972.

[4] K. Gillhousen, J. Jacobs, R. Padovani, A. Viterbi, L. Weaver, and C. Wheatley, "On the capacity of a cellular CDMA system," *IEEE Trans. Veh. Technol.*, vol. 40, pp. 303–312, May 1991.

[5] S. Verdu, "Minimum probability of error for Gaussian multiple-access channels," *IEEE Trans. Inform. Theory*, vol. IT-32, pp. 85–96, Jan. 1986.

[6] Z. Xie, C. Rushforth, and R. Short, "Multi-user signal detection using sequential decoding," *IEEE Trans. Commun.*, vol. 38, pp. 578–583, May 1990.

[7] M. Varanasi and B. Aazhang, "Near-optimum detectors in synchronous code division multiple-access systems," *IEEE Trans. Commun.*, vol. 39, pp. 725–736, May 1991.

[8] G. Turin, "Effect of multipath and fading on the performance of direct sequence CDMA systems," *IEEE J. Select. Areas Commun.*, vol. 2, pp. 597–603, July 1984.

[9] K. Schneider, "Optimum detection of code division multiplexed signals," *IEEE Trans. Aerosp. Electron. Syst.*, vol. AES-15, pp. 181–185, Jan. 1979.

[10] S. Wijayasuriya, "Alleviation of near-far effects in DS-CDMA mobile radio," Ph.D. dissertation, University of Bristol, U.K., 1993.

[11] M. Varanasi and B. Aazhang, "Multi-stage detection in asynchronous code-division multiple-access communications," *IEEE Trans. Commun.*, vol. 38, pp. 509–519, Apr. 1990.

[12] A. Viterbi, "Very low rate convolutional codes for maximum theoretical performance of spread spectrum multiple access channels," *IEEE J. Select. Areas Commun.*, vol. 8, pp. 641–649, 1990.

[13] P. Dent, B. Gudmundson, and M. Ewerbring, "A novel code division multiple access scheme based on interference cancellation," in *Int. Symp. Personal, Indoor, and Mobile Radio Commun.*, Boston, MA, Oct. 1992, pp. 98–102.

[14] R. S. Mowbray, R. D. Pringle, and P. M. Grant, "Increased CDMA capacity through adaptive cochannel interference regeneration and cancellation," *IEE Proc. I*, vol. 139, pp. 515–524, Oct. 1992.

[15] R. Lupas and S. Verdu, "Linear multi-user detectors for synchronous code division multiple-access channels," *IEEE Trans. Inform. Theory*, vol. 35, pp. 123–136, Jan. 1989.

[16] A. Duel-Hallen, "Decorrelating decision feedback multiuser detector for synchronous code division multiple access channels," *IEEE Trans. Commun.*, vol. 41, pp. 285–290, Feb. 1993.

[17] S. S. H. Wijayasuriya, G. H. Norton, and J. P. McGeehan, "Novel algorithms to solve complexity issues of decorrelation in DS-CDMA mobile radio," submitted to *IEE Proc. I.*

[18] ——, "A sliding window decorrelating algorithm for multi-user DS-CDMA systems," in *Globecom '92*, Orlando, FL, Dec. 1992, pp. 1331–1338.

[19] Z. Xie, R. T. Short, and C. K. Rushforth, "A family of suboptimum detectors for coherent multiuser communications," *IEEE J. Select. Areas Commun.*, vol. 8, pp. 683–690, May 1990.

[20] J. Lodge and M. Moher, "Maximum likelihood sequence estimation of CPM signals transmitted over rayleigh flat fading channels," *IEEE Trans. Commun.*, vol. 38, June 1990.

[21] G. H. Norton and S. S. H. Wijayasuriya, "New properties of convolutional codes and their application to communication systems," *Proc. Royal Society–pt. A.*, p. 447, 1994.

[22] S. U. H. Qureshi, "Adaptive equalization," *Proc. IEEE*, vol. 73, pp. 1349–1387, Sept. 1985.

[23] M. Varanasi and B. Aazhang, "Optimally near-far resistant multiuser detection in differentially coherent synchronous channels," *IEEE Trans. Inform. Theory*, vol. 37, pp. 1006–1018, July 1991.

[24] W. C. Y. Lee, Ed., *Mobile Cellular Telecommunications Systems.* New York: McGraw-Hill, 1990.

[25] J. G. Proakis, *Digital Communications.* New York: McGraw-Hill, 1989.
[26] R. Price and P. E. Green, "A communication technique for multipath channels," *Proc. IRE,* vol. 46, pp. 555–570, Mar. 1958.
[27] A. Turkmani, D. Demery, and J. Parsons, "Measurement and modeling of wide band mobile radio channels at 900 MHz," *IEE Proc. I.,* vol. 138, pp. 447–457, Oct. 1991.
[28] S. S. H. Wijayasuriya, G. H. Norton, and J. P. McGeehan, "Analysis of sliding window decorrelation in DS-CDMA mobile radio," *Proc. Royal Society–pt. A.*, p. 447, 1994.
[29] U. Madhow and M. Honig, "Error probability and near far resistance of minimum mean squared error interference suppression scheme for CDMA," in *Globecom '92,* Orlando, FL, Dec. 1992, pp. 1339–1343.
[30] H. Stone, "An efficient parallel algorithm for the solution of a tri-diagonal linear system of equations," *J. Assoc. Comput. Mach.,* vol. 20, pp. 27–38, Jan. 1973.
[31] G. Golub and C. Van-Loan, *Matrix Computations.* Baltimore, MD: John Hopkins University Press, 1989.
[32] Z. Zvonar and D. Brady, "On multiuser detection in asynchronous CDMA flat rayleigh fading channels," in *Int. Symp. Personal, Indoor, and Mobile Radio Commun.,* Boston, MA, Oct. 1992, pp. 123–127.
[33] ——, "Coherent and differentially coherent multiuser detectors for asynchronous CDMA frequency selective channels," in *Millcom '92,* USA, Sept. 1992, pp. 442–446.
[34] M. Schwartz, W. R. Bennett, and S. Stein, *Communication Systems and Techniques.* New York: McGraw-Hill, 1966.
[35] D. L. Noneaker and M. B. Pursley, "The effects of sequence selection on DS spread spectrum with selective fading and two forms of rake reception," in *Inform. Theory Mini Conf. Globcomm '92,* Dec. 1992, pp. 66–70.
[36] M. Kavehrad and B. Ramamurthi, "Direct sequence spread spectrum with DPSK modulation and diversity for indoor wireless communications," *IEEE Trans. Commun.,* vol. 35, pp. 224–236, Feb. 1987.
[37] W. C. Jakes, Ed., *Microwave Mobile Communications.* New York: Wiley, 1974.
[38] E. A. Geraniotis and M. B. Pursley, "Performance of coherent direct sequence spread spectrum communications over specular multipath fading channels," *IEEE Trans. Commun.,* vol. 33, pp. 502–508, June 1985.
[39] J. Wang, M. Moeneclaey, and L. B. Milstein, "Prediction diversity for CDMA indoor radio communications," in *Virginia Tech's 2nd Symp. Wireless Personal Commun.,* Blacksburg, VA, June 1992.

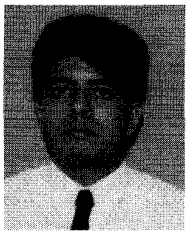

S. S. H. Wijayasuriya (S'93–M'95) was born in Colombo, Sri Lanka, in 1968. He received the B.A. Hons. degree in electronic engineering (electrical and information sciences tripos) from the University of Cambridge, U.K., in 1989 and the Ph.D. degree from the University of Bristol, U.K., in 1994.

From September 1989 to February 1991, he worked for IBM World Trade Corp. in Sri Lanka. While working toward the Ph.D. degree, he was attached to the Centre for Communications Research at the University of Bristol, where he was a Teaching Assistant and recipient of a Research Studentship in DS-CDMA mobile radio. In 1992 he was the recipient of an overseas research Student Award granted by the Committee of Vice Chancellors and Principals in the United Kingdom. He is currently the Deputy Technical Director of MTN Networks, Sri Lanka, and is closely associated with the establishment of the country's first GSM Network. His research interests include near–far resistant algorithms for DS-CDMA systems and convolutional coding techniques.

G. H. Norton was born in Cleveland, England, U.K., in 1946. He received the M.Sc. degree (with distinction) from the University of Cape Town, South Africa, in 1969 and the Ph.D. degree from Cornell University, Ithaca, NY, in 1974, also in mathematics.

From 1974 to 1984 he held various research, academic, and industrial positions in mathematics and computing. Since 1984 he has been with the Department of Electrical Engineering at the University of Bristol, England, where he is a Member of the Centre for Communications Research. His research interests are in coding theory and algebraic computing.

Dr. Norton is a member of the American Mathematical Society and a Fellow of the Institute of Mathematics and its Applications.

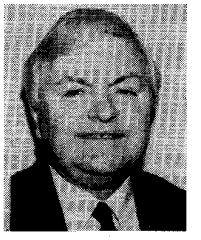

J. P. McGeehan received the B.Eng. and Ph.D. degrees in electrical and electronic engineering from the University of Liverpool, U.K., in 1967 and 1971, respectively.

In 1970 he was appointed Senior Scientist at the Allan Clark Research Centre, Plessey Company Ltd., where he was responsible for the research and development of two- and three-terminal Gunn-effect devices and their application to high-speed logic, telecommunications, and radar systems. In 1972 he became a member of the academic staff of the School of Electrical Engineering of the University of Bath, U.K., where he initiated research in the area of subsequently linear modulation for mobile radio. In November 1984, he was named Chair of Communications Engineering at the University of Bristol, U.K., and is presently Head of the Department of Electrical and Electronic Engineering and Director of the University Research Centre in Communications Engineering. He serves on numerous national and international committees concerned with mobile communications.

Dr. McGeehan is the recipient of the IEE Proceedings Mountbatten Premium and the IEEE Transactions Neal Shephard Award. He received several awards in recognition of his research contribution to radio communications from organizations, such as the Motorola Research Foundation (USA) and Schlumberger Industries (France). He is a Fellow of the IEE, the Royal Academy of Engineering, and the Royal Society of Arts and Commerce.